

PNP equations with Steric Effects: a Model of Ion Flow through Channels

Tzyy-Leng Horng

100 Wen-Hwa Rd., Seatwen
Department of Applied Mathematics
Feng Chia University
Taichung, Taiwan 40724
Email: tlhorng@math.fcu.edu.tw

Tai-Chia Lin

Department of Mathematics, National Taiwan University,
Taida Institute for Mathematical Sciences (TIMS),
No.1, Sec. 4, Roosevelt Road, Taipei 106, Taiwan
Email: tclin@math.ntu.edu.tw

Chun Liu

Department of Mathematics
Pennsylvania State University
University Park, PA 16802, USA,
Email: liu@math.psu.edu

Bob Eisenberg

Department of Molecular Biophysics and Physiology
Rush University
1653 West Congress Parkway
Chicago IL 60612 USA
Email: beisenbe@rush.edu

July 31, 2012

File Name: pnpsteric_July_31-1_2012.docx

Location: C:\Users\Bob Eisenberg\Documents\Bob Collaborators\Allen Horng and 3D PNP\Steric PNP\Referee Report\pnpsteric_July_31-1_2012.docx

Abstract

The flow of current through an ionic channel is studied using the energetic variational approach of Liu, *et al.*, applied to the primitive (implicit solvent) model of ionic solutions. This approach allows the derivation of self-consistent (Euler Lagrange) equations to describe the flow of spheres through channels. The partial differential equations derived involve the global interactions of the spheres and are replaced here with a local approximation¹, we call steric PNP (Poisson-Nernst-Planck). Kong combining rules are used and a range of values of steric interaction parameters are studied. These parameters change the energetics of steric interaction but have no effect on diffusion coefficients in model and simulations. Calculations are done for the calcium (EEEE, EEEA) and sodium channel (DEKA) previously studied in Monte Carlo simulations with comparable results. Biological function is quite sensitive to the steric interaction parameters and we speculate that a wide range of the function of channels and transporters, even enzymes, might depend on such terms. We point out that classical theories of channels, transporters, and enzymes depend on ideal representations of ionic solutions in which nothing interacts with nothing, even in the enormous concentrations found near and in these proteins, or near electrodes in electrochemical cells, for that matter. We suggest that a theory designed to handle interactions might be more appropriate. We show that one such theory is feasible and computable: steric PNP allows direct comparison with experiments measuring flows as well as equilibrium properties. Steric PNP combines atomic and macroscales in a computable formulation that allows calculation of the macroscopic effects of changes in atomic scale structures (size $\cong 10^{-10}$ meters) studied so extensively in channology and molecular biology.

Keywords

Ion channel, Poisson-Nernst-Planck equations, energetic variational approach, EnVarA, permeability, selectivity, gating, transporters, PNP, steric effects, Chebyshev pseudospectral method.

Introduction

Ion channels are protein molecules that conduct ions (like Na^+ , K^+ , Ca^{2+} , and Cl^- that might be named ‘bio-ions’ because of their universal importance in biology) through a narrow pore of fixed charge formed by the amino acids of the channel protein.² Membranes are otherwise quite impermeable to natural substances, and so channels are gatekeepers for cells, natural nanovalves that control a wide range of biological function.³ Channels open and close stochastically, allowing ionic current to flow, forming a path for solute movement, when they are open.⁴⁻⁶ Only electrodiffusion moves ions through channels, and so this biological system is like a hole in a wall that we should be able to understand physically.⁷⁻⁹

Ion channels are responsible for signaling in the nervous system, coordination of muscle contraction, and transport of dissolved substances, and water, in all tissues. Each of these functions has been so important for so long that evolution has probably produced a nearly optimal adaptation within physical constraints, and conserved it, using the same design principle again and again.

Investigation of the physical mechanisms of current flow has just begun, although there is no shortage of descriptive metaphors in the literature of structural, molecular biology and biophysics.² The fundamental problem in a physical analysis is one of scales.¹⁰ Mutations in single amino acids, that sometimes change only a handful of atoms, involving perhaps just one permanent charge (radius of ~ 0.1 nm), have dramatic biological effects. Such sensitivity comes as no surprise to the biologically oriented chemist or physicist.

Theories and simulations must account for the sensitivity of macroscopic function to atomic detail. Ion channels are nanovalves designed so a few atoms, coded by the genetic blueprint of the protein, can control macroscopic function: that is what nanovalves (and channels) are all about. Theories and simulations must deal with 0.1 nm structural changes in charged groups that produce changes on the macroscopic scale of function. Structures as small as 0.1 nm move—and cannot be stopped from moving—in thermal (nearly Brownian) motion in 10^{-16} sec. Their trajectories reverse direction ‘infinitely’ often, while biology moves on time scales of 10^{-3} second or so in much simpler trajectories. The central physical issue is how to preserve this sensitivity to tiny structures while averaging over trajectories with such complex behavior, over a 10^{13} range of time. Other scales also pose problems. Physics and biology—and simulations of physics and biology—must cope with the wide range of time scales and concentrations¹⁰ as well as the immense range and strength of the electric field.¹¹⁻¹⁵

The extremes of length, time, and concentration scales are all involved in the natural function of ion channels (or any nanovalve) so theory and simulations must deal with all these extremes together. It is not likely that atomic scale simulations, by themselves, will be able to deal with these, all together in finite time. Rather, reduced models, of the type used widely in the physical sciences, are more likely to be helpful for the foreseeable future.

A useful reduced model will include atomic scale structural variables that determine macroscopic function. Sensitivity functions, determined by the theory of inverse problems, can help evaluate and construct reduced models. Biological function will be sensitive to important parameters and insensitive to others. The utility of these models can be evaluated by solving the relevant inverse problem for channels¹⁶⁻¹⁸ using general methods.^{19,20}

So far, the most studied reduced model for ion flow in bulk and channels is the Poisson-Nernst-Planck (PNP) equation.^{11,12,21-26} Although this model has some success in dealing with experimental data.^{22,27-51} it does not include correlations introduced by the finite diameter of ions,⁵² and these are of great importance in determining the selectivity of channels^{9,53,54} and the properties of ionic solutions in general.⁵⁵⁻⁶⁹ Crudely speaking, PNP is to nonequilibrium systems (like channels) what Poisson Boltzmann is to static systems: both are first approximations, useful to show the crucial role of the electric field^{11,12,14,70}, the ionic atmosphere, and screening.⁷¹ Neither are adequate models for ionic solutions like sea water or the related solutions inside and outside biological cells.^{52,72-74}

Recently, work by Eisenberg, *et al.*,⁷⁵⁻⁷⁸—built on the energetic variational theory of complex fluids^{77,79-86}—has developed a new set of PNP equations to implement and generalize an approach to selectivity started by Nonner and Eisenberg.⁸⁷⁻⁹² Nonner and Eisenberg (*et al.*) considered a simplified model with ions (and side chains of the channel protein) represented as spheres of different finite sizes. They have shown in a long series of papers that important (static) selectivity properties of some significant types of ion channels can be explained with this model (reviewed in^{9,53,93}). They have in fact constructed a single model, with two adjustable parameters (diameter of channel, dielectric coefficient of protein, both set **only** once to unchanging values), using a **single** set of (crystal) radii of ions that fits the detailed and complex selectivity properties of two quite different types of channels, the Ca_v calcium channel^{90,94-98} of heart and the Na_v sodium channel of nerve^{9,91,99}. The theory accounts for the properties observed in solutions of different composition, with concentrations ranging from 10⁻⁷ to 0.5 Molar. When the ‘side chains’ in the model are amino acid ‘residues’ Asp-Glu-Lys-Ala, the channel has net charge of -1 although it is very salty (the magnitude of net charge is three). The channel then is a DEKA sodium channel. When the side chains are Asp-Glu-Glu-Ala, then channel is even saltier (the channel has net charge -3). It is a DEEA calcium channel, with quite different properties, **although no parameters in the model are changed whatsoever**, except the side chains that determine selectivity.

Most importantly, channels have been built according to the prescription of this theory and they behave as predicted.¹⁰⁰⁻¹⁰² Studying another channel, the ryanodine receptor (of enormous biological importance as the final regulator of Ca²⁺ concentration in muscle and thus of contractions), Gillespie, *et al.*, have successfully predicted subtle and complex properties of selectivity and permeation before experiments were done. Gillespie, *et al.*, predicted the properties of drastic mutants in a wide range of solutions before the experiments were performed,¹⁰³⁻¹¹² extending work on an earlier unsuccessful reduced model of the receptor that did not deal with the finite diameter of ions.^{30,32,113,114} One of the

Meissner/Gillespie mutants reduces the permanent charge from 13 M to zero, and yet Gillespie's theory fits current voltage relations in several solutions with nearly the same ~ 8 parameters as wild type.

The calculations reported here extend the pioneering calculations of Hyon^{75,76,78} applying the energy variational approach to ion channels.¹¹⁵ The treatment of the baths and boundary conditions are somewhat different. A full three dimensional treatment is needed before the appropriate one dimensional approximation (particularly boundary conditions) can be determined without ambiguity.^{25,43,88,116-121}

Here, we simulate the properties of the family of calcium channels Cav (reviewed in^{9,98}) and sodium channels Nav^{91,99} using parameters already shown to fit a wide range of stationary (time independent) experimental data in a variety of 'symmetrical' solutions, solutions designed so current does not flow. Our results agree with previous equilibrium binding results and extend them to the world of current voltage relations using a model and numerical methods that can be easily implemented on inexpensive computers. Current voltage relations compute in a few hours of time on a notebook system.

Mathematical model

Poisson-Nernst-Planck (PNP) equations with size effects. The energy functional and the procedures for handling it with the variational calculus are central to the Energetic Variational Approach (EnVarA) formulated by Chun Liu, more than anyone else. Liu's approach is described in references.^{75,79-82,84,115,122-126} The 'energy' of EnVarA is shown to correspond to the Helmholtz free energy of classical thermodynamics (in applicable equilibrium systems) in the recent article¹²⁷. The application of EnVarA to membranes¹²⁸, biological cells and tissues⁷⁷, and ions—in channels and bulk solution—is described in detail in references,^{1,75-78} hopefully in a way accessible to physicists and chemists without extensive experience with variational methods.

The energy functional for the ion channel is defined by

$$E = \int \left(k_B T \sum_{i=1}^N c_i \log c_i + \frac{1}{2} \left(\rho_0 e + \sum_{i=1}^N z_i e c_i \right) \phi + V c_{O^{-1/2}} \right) d\bar{x} \\ + \sum_{i=1}^N \sum_{j=1}^N \iint \frac{\epsilon_{ij} (a_i + a_j)^{12}}{2 |\bar{x} - \bar{y}|^{12}} c_i(\bar{x}) c_j(\bar{y}) d\bar{y} d\bar{x} \quad (1)$$

where c_i , z_i are concentration and valence for i^{th} ion ($i = 1, \dots, N-1$); $c_N = c_{O^{-1/2}}$ is the concentration for side chain $O^{-1/2}$ (as in the glutamate side chain) with valence $z_N = z_{O^{-1/2}} = -\frac{1}{2}$ located in the filter only; ϕ is the electrostatic potential; k_B is the Boltzmann constant; T is the absolute temperature; N is the number of ions; e is the unit charge; ρ_0 is the permanent charge density; $c_{O^{-1/2}}$ is the concentration for the spherical 'side chain' with valence $z_{O^{-1/2}} = -\frac{1}{2}$ located in the filter only; V is the

restraining potential that keeps the side chain inside the filter at all times; a_i and a_j are radii for ion i and j ; ε_{ij} is then energy coupling constant between ion i (including side chain $O^{-1/2}$) and j (including side chain $O^{-1/2}$). The last term is the repulsive part of the hard sphere potential that keeps ions apart.

The hard sphere repulsion characterizes the finite-size effect of ions and side chains inside the filter. These repulsive terms obviously depend on the chemical species and are called combining rules when they describe interactions of different species. We discuss the combining rules later.

The basic reasoning is that the ion filter is so narrow that extra energy is needed to crowd ions into its tiny volume.^{9,53,54,87,89,95-97,99,101,102,104,129-131} Without finite size effects, the total energy will yield the traditional PNP equations.

The Euler-Lagrange equations of eq. (1) will introduce the PNP equations with size effects that depend on the global properties of the problem, in the following way

$$-\nabla \cdot (\varepsilon \nabla \phi) = \rho_0 e + \sum_{i=1}^N z_i e c_i, \quad (2)$$

$$\frac{\partial c_i}{\partial t} + \nabla \cdot \vec{J}_i = 0, \quad (3)$$

where flux \vec{J}_i is

$$\vec{J}_i = -D_i \nabla c_i - \frac{D_i c_i}{k_B T} z_i e \nabla \phi - \frac{D_i c_i}{k_B T} \sum_{j=1}^N \nabla \int \frac{\varepsilon_{ij} (a_i + a_j)^{12}}{|\vec{x} - \vec{y}|^{12}} c_j(\vec{y}) d\vec{y}, \quad \text{for } i = 1, \dots, N-1 \quad (4)$$

There is extra flux from the restraining potential that keeps side chains within the selectivity filter

$$\vec{J}_N = -D_N \nabla c_N - \frac{D_N c_N}{k_B T} z_N e \nabla \phi - \frac{D_N c_N}{k_B T} \nabla V - \frac{D_N c_N}{k_B T} \sum_{j=1}^N \nabla \int \frac{\varepsilon_{Nj} (a_N + a_j)^{12}}{|\vec{x} - \vec{y}|^{12}} c_j(\vec{y}) d\vec{y} \quad (5)$$

These equations are very similar to the drift-diffusion equations of semiconductors^{11,12,23,24,116,121,132-149} with the first term in the flux being the diffusion term and the second one being the drift term driven by electrostatic potential of the field.

The third term involves a mutual repulsive force and inter-particle hard sphere potential that is not typically found in semiconductor equations (although the semiconductor literature is so large that volume exclusion of finite size holes and electrons is probably found somewhere we do not know). This term includes forces usually called ‘Lennard Jones’ and depends globally on the properties of the solution everywhere, because of the range of the integral on the right hand side of eq. (4) and (5).

We call attention to the important role that the coefficients of these steric terms will have in determining biological function. The role of these steric terms will be somewhat different in our calculations from those in classical equilibrium analysis of ionic solutions using Monte Carlo simulations, for example. The cross terms in our expression appear as part of partial differential equations. These terms will then have effects on all terms *in the solution* of those partial differential equations. The integration process ‘spreads out’ the effects of the cross terms. They propagate into everything as the partial differential equations are solved. The usual classical equilibrium treatment of Monte Carlo simulations is likely to produce different radial distribution functions different from those produced by our differential equations, but detailed comparison of MC and EnVarA calculations of absolutely identical models is necessary to check the significance (or even existence) of this effect.

The steric cross terms—often called combining rules—turn out to have significant effects on the properties of ion channels. As mentioned, we use the Kong combining rules,¹⁵⁰ to describe repulsion between ionic spheres, since they seem more accurate and justified^{151,152} than the more common Lorentz-Berthelot rules. It will turn out that the biological properties of ion channels are quite sensitive to these terms, but the choice of parameters seems to require detailed fitting to the properties of specific biological channels and transporters. We do not know what the effects of attractive terms (known to be present in bulk solutions) will be when we include them. We reiterate that these terms do not change diffusion coefficients in our model.

One might think that simulations in full atomic detail (of molecular dynamics) would give good estimates of combining rules, but sadly that is not the case. These simulations of molecular dynamics use combining rules (similar or identical to what we use in our reduced models) in the force fields of their own calculations. Without particular justification beyond that provided in standard references,¹⁵⁰⁻¹⁵² we cannot use molecular dynamics to justify (or check) our combining rules that it also assumes as much as we do. It is possible that no one knows what cross terms to use in bulk solution. It seems likely that no one knows what cross terms should be used inside a channel, or between side chains and ions. Indeed, it is difficult to conceive of experiments that might measure these inside channels with reasonable reliability. (We suspect, from several conversations, that designers of force fields for molecular dynamics simulations have no more idea how to calibrate combining rules, inside a protein, or perhaps anywhere, than we do.)

Returning to the mathematical issues, we note that the singular convolution integral term can be regularized by a cut-off in integration domain or simply letting the integrand be 0 when $|\vec{x} - \vec{y}| \leq a_i + a_j$. However, the regularized term still produces numerical difficulty and is very time-consuming to compute, particularly in high dimensions, even if fast Fourier transform methods are used. We have tried.

In addition, computing the convolution term generates an *artificial* boundary layer with length of several grid spacings that needs to be filtered out and may have troublesome *qualitative* effects not so easy to remove by any local filtering since it has some of the properties of aliasing. Aliasing has devastating effects if not handled properly in both temporal and spatial systems which are treated as periodic when they are not.

We turn now to a simplified steric model that is much easier to compute because it uses only a local representation of interatomic forces. As we shall see, this steric model allows computation of a large range of interesting phenomena, despite this simplification.

Local PNP equations with steric effects (PNP-steric equations)

$$\vec{J}_i = -D_i \nabla c_i - \frac{D_i c_i}{k_B T} z_i e \nabla \phi - \frac{D_i c_i}{k_B T} \sum_{j=1}^N \varepsilon_{ij} \delta^{-12+d} (a_i + a_j)^{12} \nabla c_j, \quad i = 1, \dots, N-1 \quad (6)$$

$$\vec{J}_N = -D_N \nabla c_N - \frac{D_N c_N}{k_B T} z_N e \nabla \phi - \frac{D_N c_N}{k_B T} \nabla V - \frac{D_N c_N}{k_B T} \sum_{j=1}^N \varepsilon_{Nj} c_\delta \delta^{-12+d} (a_N + a_j)^{12} \nabla c_j \quad (7)$$

where δ is a small number for the cut-off length and c_δ is a dimensionless integrating factor associated with δ and d is dimension. Here the symmetry $\varepsilon_{ij} = \varepsilon_{ji}$ has been assumed for notational convenience. To get this model, we have two important considerations: 1) the localization of the nonlocal size effects, and 2) the finite truncations, which make the term local. Compared to the standard PNP equations, the PNP-steric equations have extra nonlinear differential terms (in the spatial variables) called steric effects. These represent the effective averaging/coarse graining of microscopic size effects for the macroscopic/continuum scales.

It should be clearly understood that coarsening terms of this sort are used throughout the chemistry literature, including within the simulations of molecular dynamics. The ‘potentials’ of molecular dynamics simulations of proteins are not transferrable from quantum mechanical simulations of interatomic forces. The force fields that are used in every time step of an atomic scale simulation include terms like our ε_{ij} justified only the way we have. Thus, molecular dynamics simulations depend on effective parameters as do ours. Molecular dynamics simulations are no more derivable from quantum mechanics, for example, than are our models.

The main difficulty of the equations (2)-(5) comes from the convolution integral of the energy functional E with the following form

$$\iint \frac{1}{|\vec{x}-\vec{y}|^{12}} c_i(\vec{x}) c_j(\vec{y}) d\vec{y} d\vec{x} \quad (8)$$

Usually one would approximate the above integral by truncating the kernel $1/|\bar{x} - \bar{y}|^{12}$ with the cut off length δ which makes the kernel $1/|\bar{x} - \bar{y}|^{12}$ have a flat-top when $|\bar{x} - \bar{y}| \leq \delta$. To approach the kernel $1/|\bar{x} - \bar{y}|^{12}$, the length δ must be set as a small number tending to zero. One may expect that the smaller the cut-off length δ , the better the approximation. However, due to the effect of high-frequency Fourier modes, the approximation may lose the accuracy of numerical computations and makes numerical simulations difficult and inefficient.¹⁵³

To deal with the effect of high-frequency Fourier modes, band-limited functions are used to cut off high-frequency Fourier modes. The functions act like optical filters selectively transmitting light in a particular range of wavelengths. Band-limited functions play important roles in the design of signal transmission systems with many applications in engineering, physics and statistics.¹⁵⁴ See also any textbook on digital signal or image processing. In reference,¹ a class of band-limited functions depending on the length δ is found to approximate the kernel $1/|\bar{x} - \bar{y}|^{12}$ and allow the derivation of the PNP-steric equations. The same approach can be used to modify the Poisson-Boltzmann equations used widely in physical chemistry, applied mathematics, and molecular biology.^{70,155} Once modified, these new steric Poisson-Boltzmann equations are particularly useful for the study of crowded boundary layers near charged walls, including the special behavior usually attributed to Stern layers. As the length δ goes to zero, the singular integral (8) can be approximated by the integral $S_\delta \int c_i(\bar{x})c_j(\bar{x})d\bar{x}$ with $S_\delta \sim \delta^{-12+d}$. Hence, the energy functional (1) can also be approximated by

$$E_\delta = \int \left(k_B T \sum_{i=1}^N c_i \log c_i + \frac{1}{2} \left(\rho_0 e + \sum_{i=1}^N z_i e c_i \right) \phi + V c_{O^{-1/2}} \right) d\bar{x} + \sum_{i,j=1}^N \frac{g_{ij}}{2} \int c_i(\bar{x})c_j(\bar{x})d\bar{x}$$

which gives the equations (2), (3), (6) and (7), where $g_{ij} = \varepsilon_{ij} (a_i + a_j)^{12} S_\delta$ for $i = 1, \dots, N-1$, and $g_{Nj} = \varepsilon_{Nj} (a_i + a_j)^{12} c_\delta S_\delta$.

The PNP-steric equations (2), (3), (6) and (7) are convection-diffusion equations having the energy dissipation law:

$$\frac{d}{dt} E_\delta = - \int \sum_{i=1}^N \frac{D_i c_i}{k_B T} \left| \nabla (k_B T \log c_i + z_i e \phi + \mu_i) \right| ,$$

where $\mu_i = \sum_{j=1}^N g_{ij} c_j$ is the chemical potential.

Note that the equations (6) and (7) contain no singular integrals like the equations (4) and (5) but have extra nonlinear differential terms. These extra nonlinear terms are crucial to simulate the selectivity of ion channels that cannot be found by simulating the standard PNP equations. Hence, the (local)

PNP-steric equations are more useful than the standard PNP equations and are significantly more efficient and easy to work with than the global equations of the EnVarA treatment (2)-(5) discussed in the Introduction and Discussion sections of this paper. These extra local terms in differential equations (6) and (7) have global effects when the differential equations are solved. Thus, pair correlation functions described by solutions to differential equations (4) & (5) may have properties not present in classical equilibrium analyses containing local steric forces. (Classical analyses often deal only with forces and not with solutions of differential equations containing the forces.) Detailed fitting to specific experimental data is needed to compare the solutions of the local steric *differential* equations (6) and (7); the solutions of the more general differential equations (4) and (5); and the actual nonlocal phenomena of experiments.

We adopt the PNP-steric equations. We replace eq.'s (4) & (5) with the more approximate eq.'s (6) & (7) from now on. The real three dimensional geometry of an ion channel shown in Fig. 1 is replaced with a simple axis-symmetric geometry shown Fig. 2 with the eqs. (2), (3) and (6) valid in Ω , and eq. (7) valid *only* in Ω_f , where Ω_f is the filter part of channel and $\Omega_f \subset \Omega$. The associated boundary conditions are also shown in Fig. 2 with Dirichlet boundary conditions specified for both ionic concentration and potential at channel's inlet (left end) and outlet (right end); no-flux boundary conditions are set for both ionic concentration and potential at the side-wall of channel. Extra no-flux boundary conditions are set for the side chains $J_{O^{-1/2}} = 0$ at the interfaces ($z = \alpha$ and β) between filter and the other part of channel, since side chain molecules are only free to move inside the filter.

This model is meant to be nearly identical to that used in the many papers using Monte Carlo methods reviewed in reference⁹ particularly the key papers.^{54,90,93-96,99,156} The treatment of the region outside the channel and thus buildup phenomena are different from those in references.^{75,76,78}

Since no-flux boundary conditions are implemented for both ionic concentration and potential at the side walls (orthogonal to the direction of current flow), this two dimensional problem, eqs. (2), (3) (6) and (7), can be well approximated by a reduced one dimensional problem along the axial direction z , with cross-section area factor $A(z)$ included as done in references^{25,43,88,116-121} described succinctly in reference¹¹⁹ and perhaps most carefully in the three dimensional spectral element calculations of Hollerbach.^{34,43} Of course, some phenomena cannot be reproduced well in one dimension. See Fig. 7 of reference.⁹⁹

The resulting one dimensional equations are

$$-\frac{1}{A} \frac{d}{dz} \left(\varepsilon A \frac{d\phi}{dz} \right) = \rho_0 e + \sum_{i=1}^N z_i e c_i, \quad (9)$$

$$\frac{\partial c_i}{\partial t} + \frac{1}{A} \frac{\partial}{\partial z} (A J_i) = 0, \quad (10)$$

$$\vec{J}_i = -D_i \frac{\partial c_i}{\partial z} - \frac{D_i c_i}{k_B T} z_i e \frac{\partial \phi}{\partial z} - \frac{D_i c_i}{k_B T} \sum_{j=1}^N \varepsilon_{ij} \delta^{-9} (a_i + a_j)^{12} \frac{\partial c_j}{\partial z}, \quad i=1, \dots, N-1 \quad (11)$$

$$\vec{J}_N = -D_N \frac{\partial c_N}{\partial z} - \frac{D_N c_N}{k_B T} z_N e \frac{\partial \phi}{\partial z} - \frac{D_N c_N}{k_B T} \sum_{j=1}^N \varepsilon_{Nj} c_\delta \delta^{-9} (a_N + a_j)^{12} \frac{\partial c_j}{\partial z} - \frac{D_N c_N}{k_B T} \frac{dV}{dz} \quad (12)$$

with boundary and interface conditions

$$c_i(0, t) = c_i^L, \quad \phi(0, t) = \phi^L, \quad c_i(a, t) = c_i^R, \quad \phi(a, t) = \phi^R. \quad (13)$$

$$\vec{J}_N(\alpha, t) = \vec{J}_N(\beta, t) = 0. \quad (14)$$

The no-flux interface conditions for the side chains guarantee that side chains are not allowed to leave the filter. Mass conservation is preserved inside the filter:

$$\frac{d}{dt} \int_{\alpha}^{\beta} A(z) c_{O^{-1/2}}(z, t) dz = 0, \quad \forall t.$$

Also, in eqs. (11)-(12), the Einstein relation is used for both drift current and hard-sphere-potential flux, which is $\mu_{e,i} = D_i/k_B T$, $\mu_{LJ,i} = D_i/k_B T$ ($i=1, \dots, N-1$), $\mu_{V,N} = D_N/k_B T$, where $\mu_{e,i}$ and $\mu_{LJ,i}$ are electrical mobility and the mobility associated with hard sphere potential for ionic species i ; $\mu_{V,N}$ is the mobility associated with restraining potential for glutamate. Note that $D_i, \forall i$, do not have to be homogeneous in space. Nor do the dielectric coefficients of solution and channel protein. We have not yet studied the effects of variation in these parameters, however. Usually, $D_i, \forall i$, is set to $1/20^{th}$ of its bulk solution value inside the channel filter, while set to bulk solution value in the rest of channel as discussed at length in the supplementary material and body of reference.¹⁰⁹

Dimensionless equations Non-dimensionalization of governing equations is especially important in discovering the structure, such as boundary or internal layer, of the solution of PNP type equations, in advance, and so perturbation methods^{21,24,25,135,157}—including now some using the powerful and rigorous methods of geometrical perturbation theory^{24,147,148}—have been used. We follow this work, and scale the dimensional variables by physically meaningful quantities.

$$\begin{aligned} \tilde{c} &= \frac{c_i}{c_{\max}}, \quad \tilde{\rho}_0 = \frac{\rho_0}{c_{\max}}, \quad \frac{\phi}{k_B T / e} = \tilde{\phi}, \quad \frac{\varepsilon_{ij}}{k_B T} = \tilde{\varepsilon}_{ij}, \quad \frac{V}{k_B T} = \tilde{V}, \\ &: \\ \tilde{s} &= \frac{s}{L}, \quad \tilde{\delta} = \frac{\delta}{L}, \quad \tilde{A} = \frac{A}{L^2}, \quad \tilde{t} = \frac{t}{L^2 / D_{Na}}, \quad \tilde{D}_i = \frac{D_i}{D_{Na, \text{bulk}}}, \end{aligned}$$

where s denotes all length scale, and $L = r_{\min}$ (the narrowest radius in channel shown in Fig. 2) unless specified otherwise. Note the scaling with respect to the physical dimension and not to the Debye length. The Debye length varies with concentration and concentration varies with location and

conditions. Eq. (8) becomes

$$-\frac{1}{\tilde{A}} \frac{\partial}{\partial \tilde{z}} \left(\Gamma \tilde{A} \frac{\partial \tilde{\phi}}{\partial \tilde{z}} \right) = \tilde{\rho}_0 + \sum_{i=1}^N z_i \tilde{c}_i, \quad (15)$$

where $\Gamma = \lambda^2/L^2$, and the Debye length $\lambda = \sqrt{\varepsilon k_B T / c_{\max} e^2}$. Γ is the reciprocal of the length of the channel in units of Debye lengths. Note that Γ can vary dramatically with location and conditions if the contents of the channel vary with location or conditions.. In the channels dealt with here, the contents of the channel are ‘buffered’ by the charge of the side chains of the protein, most clearly in the calcium channels EEEE, and EEEA, but also for the salty DEKA channel. Such buffering is not expected in all channels, e.g., potassium channels.

Eqs. (9-11) then become

$$\frac{\partial \tilde{c}_i}{\partial \tilde{t}} + \frac{1}{\tilde{A}} \frac{\partial}{\partial \tilde{z}} (\tilde{A} \tilde{J}_i) = 0, \quad (16)$$

$$\begin{aligned} \tilde{J}_i &= -\tilde{D}_i \frac{\partial \tilde{c}_i}{\partial \tilde{z}} - \tilde{D}_i \tilde{c}_i z_i \frac{\partial \tilde{\phi}}{\partial \tilde{z}} - \tilde{D}_i \tilde{c}_i \sum_{j=1}^N \tilde{\varepsilon}_{ij} c_\delta \tilde{\delta}^{-9} (\tilde{a}_i + \tilde{a}_j)^{12} \frac{\partial \tilde{c}_j}{\partial \tilde{z}} \\ &= -\tilde{D}_i \frac{\partial \tilde{c}_i}{\partial \tilde{z}} - \tilde{D}_i \tilde{c}_i z_i \frac{\partial \tilde{\phi}}{\partial \tilde{z}} - \tilde{D}_i \tilde{c}_i \sum_{j=1}^N \tilde{g}_{ij} \frac{\partial \tilde{c}_j}{\partial \tilde{z}}, \end{aligned} \quad (17)$$

$$\begin{aligned} \tilde{J}_N &= -\tilde{D}_N \frac{\partial \tilde{c}_{O^{-1/2}}}{\partial \tilde{z}} - \tilde{D}_N \tilde{c}_N z_N \frac{\partial \tilde{\phi}}{\partial \tilde{z}} - \tilde{D}_N \tilde{c}_N \sum_{j=1}^N \tilde{\varepsilon}_{Nj} c_\delta \tilde{\delta}^{-9} (\tilde{a}_N + \tilde{a}_j)^{12} \frac{\partial \tilde{c}_j}{\partial \tilde{z}} - \tilde{D}_N \tilde{c}_N \frac{d\tilde{V}}{d\tilde{z}} \\ &= -\tilde{D}_N \frac{\partial \tilde{c}_N}{\partial \tilde{z}} - \tilde{D}_N \tilde{c}_N z_N \frac{\partial \tilde{\phi}}{\partial \tilde{z}} - \tilde{D}_N \tilde{c}_N \sum_{j=1}^N \tilde{g}_{Nj} \frac{\partial \tilde{c}_j}{\partial \tilde{z}} - \tilde{D}_N \tilde{c}_N \frac{d\tilde{V}}{d\tilde{z}}. \end{aligned} \quad (18)$$

We remove all the tilde decorations \sim and rewrite the dimensionless governing equations (15)-(18) for the mixture of Na^+ , Ca^{2+} , Cl^- and $\text{O}^{-1/2}$ as follows:

$$-\frac{1}{A} \frac{\partial}{\partial z} \left(\Gamma A \frac{\partial \phi}{\partial z} \right) = \rho_0 + z_{O^{-1/2}} c_{O^{-1/2}} + z_{\text{Na}} c_{\text{Na}} + z_{\text{Ca}} c_{\text{Ca}} + z_{\text{Cl}} c_{\text{Cl}}, \quad (19)$$

$$\frac{\partial c_i}{\partial t} + \frac{1}{A} \frac{\partial}{\partial z} (A J_i) = 0, \quad i = \text{Na}^+, \text{Ca}^{2+}, \text{Cl}^- \text{ and } \text{O}^{-1/2}, \quad (20)$$

$$J_i = -D_i \frac{\partial c_i}{\partial z} - D_i c_i z_i \frac{\partial \phi}{\partial z} - D_i c_i \left(g_{i\text{Na}} \frac{\partial c_{\text{Na}}}{\partial z} + g_{i\text{Ca}} \frac{\partial c_{\text{Ca}}}{\partial z} + g_{i\text{Cl}} \frac{\partial c_{\text{Cl}}}{\partial z} + g_{i\text{O}^{-1/2}} \frac{\partial c_{\text{O}^{-1/2}}}{\partial z} \right), \quad i = \text{Na}, \text{Ca}, \text{Cl}, \quad (21)$$

$$\begin{aligned} J_{O^{-1/2}} &= -D_{O^{-1/2}} \frac{\partial c_{O^{-1/2}}}{\partial z} - D_{O^{-1/2}} c_{O^{-1/2}} z_{O^{-1/2}} \frac{\partial \phi}{\partial z} - D_{O^{-1/2}} c_{O^{-1/2}} \frac{dV}{dz} \\ &\quad - D_{O^{-1/2}} c_{O^{-1/2}} \left(g_{O^{-1/2}\text{Na}^+} \frac{\partial c_{\text{Na}}}{\partial z} + g_{O^{-1/2}\text{Ca}^{2+}} \frac{\partial c_{\text{Ca}}}{\partial z} + g_{O^{-1/2}\text{Cl}^-} \frac{\partial c_{\text{Cl}}}{\partial z} \right) \end{aligned} \quad (22)$$

Note that $\tilde{\epsilon}_{ij}c_\delta\tilde{\delta}^{-9}(\tilde{a}_i + \tilde{a}_j)^{12}$ in eq. (17) is lumped into \tilde{g}_{ij} along with $c_\delta\tilde{\delta}^{-9}$ and it is assumed to be the same for all species. The Lennard-Jones parameters $\tilde{\epsilon}_{ij}$ are obtained from literature for alike species ($i = j$), and computed by Kong's rule for unlike species ($i \neq j$). They do not change diffusion coefficients in our model or calculations.

Channel wall shape function. The wall shape function $g(z)$ in Fig. 2 can be arbitrarily specified, for

example, $g(z) = \frac{r_{\max} - r_{\min}}{(a/2)^{2p}} \left(z - \frac{a}{2}\right)^{2p} + r_{\min}$, or non-dimensionalized as

$$\frac{g(z)}{L} = \frac{r_{\max}/L - r_{\min}/L}{(a/2L)^{2p}} \left(\frac{z}{L} - \frac{a}{2L}\right)^{2p} + \frac{r_{\min}}{L}, \quad \text{or} \quad \tilde{g}(\tilde{z}) = \frac{\tilde{r}_{\max} - \tilde{r}_{\min}}{(\tilde{a}/2)^{2p}} \left(\tilde{z} - \frac{\tilde{a}}{2}\right)^{2p} + \tilde{r}_{\min},$$

We remove all the tilde decorations \sim and rewrite

$$g(z) = \frac{r_{\max} - r_{\min}}{(a/2)^{2p}} \left(z - \frac{a}{2}\right)^{2p} + r_{\min}, \quad (23)$$

In our calculation, we choose $p = 4$. The geometrical parameters are typically $a = 50\text{\AA}$, $r_{\min} = 3.5\text{\AA}$, $r_{\max} = 40\text{\AA}$, $D = D_{Na,bulk} = 1.334 \times 10^{-5} \text{ cm}^2/\text{s}$. We set $\epsilon = 30\epsilon_0$ inside the filter; in the rest of channel, $\epsilon = \epsilon_{water} = 80\epsilon_0$. For typical $c_{\max} = 100\text{ mM}$, the Debye length $\lambda = 8.48\text{\AA}$, $\Gamma = 5.87$, inside the filter; $\lambda = 13.8\text{\AA}$, $\Gamma = 15.65$, outside the filter. The above Γ 's are based on $L = r_{\min} = 3.5\text{\AA}$.

The fact that Γ **is not small** implies that no internal or boundary layer is expected in the radial (transverse) direction. However, we sometimes choose $L = a = 50\text{\AA}$, $\Gamma = 0.0288$ inside the filter; $\Gamma = 0.07668$ outside the filter. Though Γ is not then as small as in semiconductor devices, an internal/boundary layer is still expected in lateral (axial) direction. We must not forget that the non-local hard sphere potential term (present in ionic solutions but not semiconductors) may produce internal layers as well. See Fig. 7 of reference.⁹⁹

A noticeable problem in all PNP (and Poisson Boltzmann) theories without finite size are internal boundary layers near all boundaries with charge (permanent or induced). Such layers are customarily removed by introducing a **SINGLE** distance of closest approach for all ions, however ill defined. Of course, **no single distance of closest approach can deal with ions of quite different diameter**, a problem that Debye, Hückel, and Bjerrum were quite aware of, evidently. The need for multiple

distances of closest approach (different for each ion, and highly nonideal, depending on each other and everything else in the system) means that the complex layering phenomena seen near walls of charge can have counterparts in channels. Indeed, complex layering is expected when ionic solutions are mixtures, like the salt waters of oceans or biology, and spatial inhomogeneities are present. Reference¹⁵⁸ is a gateway into the enormous chemical literature on layering phenomena near walls of charge. Reference⁷⁸ is a mathematical approach. Layering in ionic solutions might be able to produce nonlinear phenomena as important as *pn* junctions or even *pnp* junctions in semiconductors.

One might argue the authenticity of choosing $r_{\min} = 3.5\text{\AA}$, and wonder if an exclusion zone adjacent to channel side wall for ion sphere center with thickness of ion radius should be put into extra consideration. In 3D models, this may be necessary, and requests extra care in computation because the radial exclusion zone is different for ions of different size or charge: see Fig. 7 of reference⁹⁹. However, in the 1D continuum model studied here, which ignores such ion specific radial effects, our single radial zone would only change the value of r_{\min} . Since all the governing equations are scaled to be dimensionless, the effect of changing r_{\min} would only change the value of Γ in eq. (19). That in turn would only change the distribution of electric potential. Γ is proportional to $1/r_{\min}^2$. The permanent charge concentration ρ_0 in eq. (19) is also proportional to $1/r_{\min}^2$. The net effect is simply reduced to the amplification or shrinking of the influence of contribution of electric potential exerted by ion distributions. The permanent charge concentration ρ_0 is generally much larger than all ion concentrations and dominates the distribution of electric potential, we imagine. We then reason that minor change of r_{\min} would not affect our results significantly.

Numerical methods Now we apply the multi-block Chebyshev pseudospectral method¹⁵³ together with the method of lines (MOL) to solve eqs. (19)-(22) with the associated boundary/interface conditions eqs. (13)-(14). These governing equations are semi-discretized in space together with boundary/interface conditions.

The resulting PNP delta representation is a set of coupled ordinary differential algebraic equations (ODAE's). The algebraic equations come from the boundary/interface conditions which are time-independent. The resulting ODAE's are index 1, which can be solved by many well-developed ODAE solvers. For example, **ode15s** in MATLAB is a variable-order-variable-step index-1 ODAE solver, that can adjust the time-step to meet the specified error tolerance, and integrate with time efficiently. The numerical stability in time is automatically assured at the same time. The spatial discretization here is performed by the highly-accurate Chebyshev pseudospectral method with Chebyshev Gauss-Lobatto grid and its associated collocation derivative matrix. To cope with the computational domain of side chains being strictly within the region $[\alpha, \beta]$, and the conformation of

grids, we need to use domain decomposition. We decompose the whole domain into $[0, \alpha]$, $[\alpha, \beta]$ and $[\beta, a]$.

The extra interface conditions from this domain decomposition for ions are implemented simply, by continuity of ion concentration and the associated flux. Finally, the Poisson equation for electric potential is solved by direct inverse at every time step, which is easy since it is only one-dimensional.

Results

Here we consider a calcium channel (EEEE) with 4 glutamate side chain, 8 $O^{-1/2}$ particles, free to move inside the filter, essentially the model introduced by Nonner and Eisenberg^{53,87-89} and used by them and their collaborators since then (reviewed in references^{9,72}). Our goal is to demonstrate the feasibility of a PNP-steric model and the range of phenomena that can be calculated despite its local approximation. Note that the effects of a local approximation on the right hand side of partial differential equations is not the same as the effects of a local approximation in a classical analysis of the BBGKY hierarchy. The much needed detailed comparison with experimental results lies in the future. We are particularly interested in the effects of the steric parameters we call ε_{ij} in eq. 1, and then the effects of g_{ij} as well, so we concentrate on steady state results. Transients of the type previously reported⁷⁵ have been computed and will be reported separately.

The channel geometry used for the current 1D simulations is shown in Fig. 3, and the parameters used are shown below. These parameters are not changed in the calculations, e.g., the diffusion coefficients are always the same and are not changed as interaction (Kong) parameters are changed.

Parameters

Filter radius: 3.5 Å. Filter length: 10Å. Diffusion coefficients in cm^2/s : non-filter region: $D_{Na^+} = 1.334e-5$, $D_{Ca^{2+}} = 0.792e-5$, $D_{Cl^-} = 2.032e-5$, $D_{O^{-1/2}} = 0.76e-5$. Filter region: diffusion coefficients 1/20 of the above values (see Gillespie¹⁰⁹ particularly Supplementary material). Ion radii: $a_{Na^+} = 0.95\text{Å}$, $a_{Ca^{2+}} = 0.99\text{Å}$, $a_{Cl^-} = 1.81\text{Å}$, $a_{O^{-1/2}} = 1.4\text{Å}$. Relative dielectric constant: 30 in the filter region, 80 in the non-filter region.

Dimensionless restraining potential for $O^{-1/2}$ inside the filter required by eq. (22):

$$V = V_{\max} \gamma (z - 0.5a)^2 \quad (24)$$

where γ is a scaling constant that makes V reach V_{\max} at $z = \alpha$ and β . Boundary conditions are:

Boundary Conditions

Voltage at both reservoirs: 100 mV. Na^+ concentration in both reservoirs: 100 mM. Ca^{2+} concentration at both reservoirs: 0.001 to 10 mM. Cl^- concentration at both

reservoirs is chosen to keep the whole solution electrically neutral.

To measure selectivity, as it is reported in the biological literature of calcium channels, we need to compute the Ca binding ratio:

$$\text{Binding ratio} = \frac{\text{Number of Ca}^{2+} \text{ ion inside the filter}}{\text{Number of Na}^+ \text{ ion inside the filter} + \text{Number of Ca}^{2+} \text{ ion inside the filter}} \quad (25)$$

Turning to the precise description of the spherical ions, we need to specify many ‘Lennard Jones’ style parameters. There are 10 parameters of the g_{ij} ’s that must be chosen, without specific experimental data relevant to the interior of a channel. (We note that this problem is not ours alone. The same situation is faced for any atomic scale model. No one knows how to choose the force fields of molecular dynamics suitable for the special conditions inside an ion channel. If one follows the convention of molecular dynamics, and use force fields that depend only on the distance between two atoms, this problem is particularly serious. Note that dielectric boundary forces are almost always of great importance in confined systems like ion channels.^{159,160} It is not likely that dielectric boundary forces acting on two ions can be well approximated as a function of *only* the distance between two ions.)

We use the energy well ϵ_{ij} data from the traditional Lennard-Jones (12-6 rule) potential as a reference. From the work of^{151,152}, we choose $\epsilon_{Na,Na} : \epsilon_{Cl,Cl} : \epsilon_{Ca,Ca} : \epsilon_{O,O} = 1 : 1 : 1 : 1.56$. Kong’s combining rule¹⁵⁰ seems the best for ionic solutions^{151,152}, with $\sigma_{ij} = (a_i + a_j)$. This gives us the ϵ_{ij} ’s for the rest of the cross hard-sphere potential terms.

$$\begin{array}{l} \epsilon_{Na,Na} : \epsilon_{Cl,Cl} : \epsilon_{Ca,Ca} : \epsilon_{O,O} : \epsilon_{Na,Cl} : \epsilon_{Na,Ca} : \epsilon_{Na,O} : \epsilon_{Cl,Ca} : \epsilon_{Cl,O} : \epsilon_{Ca,O} \\ = 1 : 1 : 1 : 1.56 : 0.955 : 1.00 : 1.28 : 0.961 : 1.21 : 1.28 \end{array}$$

and similarly

$$\begin{array}{l} g_{Na,Na} : g_{Cl,Cl} : g_{Ca,Ca} : g_{O,O} : g_{Na,Cl} : g_{Na,Ca} : g_{Na,O} : g_{Cl,Ca} : g_{Cl,O} : g_{Ca,O} \\ = 1 : 2280 : 1.64 : 164 : 42.2 : 0.642 : 8.20 : 50.4 : 327 : 10.0 \end{array}$$

We can see that $g_{Cl,j}$ (especially $g_{Cl,Cl}$) are much larger than the other g_{ij} ’s because their additional size is increased so dramatically by the exponent in $(a_i + a_j)^{12}$. These large values would make the governing equations very stiff in numerical properties and hard to integrate in time. To resolve this numerical difficulty, we remove all the hard sphere forces involving Cl^- , which means $g_{Cl,j} = 0, \forall j$. This approach can be rigorously justified because Cl^- is usually very dilute inside the filter, as are all

co-ions in ion exchangers¹⁶¹, because of the electrostatic repulsion from the highly concentrated permanent charge of eight $O^{-1/2}$.

Choosing self coupling coefficients $g_{Na,Na}$: The above coupling terms g_{ij} 's are derived as ratios, and we still need to determine actual g_{ij} 's by choosing the 'self' quantities $g_{Na,Na}$. The self-coupling $g_{Na,Na}$ is only known from its relationship to its effective ion radius: it is proportional to $(a_{Na} + a_{Na})^{12}$. Larger $g_{Na,Na}$ implies stronger hard sphere potential and more pushing among particles. Smaller $g_{Na,Na}$ implies less interaction and pushing among particles. If we choose $g_{Na,Na}$ too small, the finite-size effect will be trivial and (judging from previous work cited above), the correct selectivity of calcium ion will not be found. If we choose $g_{Na,Na}$ too large, repulsion will be too strong and the profile of concentration of all species (inside the filter) will be flat. Selectivity, as biology knows it, will not be present.

A numerical experiment (Fig. 4 and Table 1) shows how $g_{Na,Na}$ changes the Ca binding ratio. Conditions of each case are stated in figure captions. Note that many of the cases considered below correspond to different physiological states that may have profound implications for function. Cycling between such states has been the explanation of most behavior of channels and transporters for some 60 years, since Hodgkin and Huxley (who, one notes, did not use such explanations themselves). But the states in those explanations are *ad hoc*, arising as inputs of models from wisdom and experimentation on macroscopic systems, not from direct physical knowledge of channels. The states shown here in our calculations arise without human intervention or wisdom. Rather, they arise as outputs of direct self-consistent calculation. Sometimes it is better to be wise, sometimes it is not. The choice between handcrafted traditional models of states and direct calculations of ions that are sometimes in definite states should be made, in our view, by success or failure in explaining and predicting experimental results with models. The models should be parsimonious and specific, of course, so they can be falsified, at least in principle. Otherwise, they are more poetry than science.

We can summarize the observations in the following.

- (1) From eqs. (21) & (22), the flux of ion species consists of diffusion, migration (i.e., electrostatic drift driven by electric potential), and particle-to-particle steric-effect interaction. The typical steric-effect flux $-\tilde{D}_i \tilde{c}_i \tilde{g}_{ij} \frac{\partial \tilde{c}_j}{\partial z}$ can be seen as a chemical-potential drift exerted on ion species i by species j , in which $i = j$ is also allowed. The steric-effect flux generally includes a flux coupling between species i and j , and this coupling is not captured in plain PNP and DFT-PNP theory, where fluxes of one species are driven *only* by gradients of the chemical potential of that one species. Here 'everything interacts with everything else': the flux of one species is driven by gradients of the chemical potential of another species, even though we use (nearly) the same constitutive (NP) relation for transport as in classical PNP or DFT-PNP. Our chemical-potential drift term is not like

electrostatic drift. The electrostatic drift can flow uphill or downhill along the electric potential, depending on the sign of the valence z_i being negative or positive. The chemical potential drift, on the other hand, **always flows downhill** along the chemical potential unless $\tilde{D}_i \tilde{g}_{ij}$ is negative, which is impossible if particle-to-particle steric-effect interaction is always repulsive (not attractive). If particles push each other away, peaks of ion concentrations (of different species) tend to separate from each other as best they can, unless frustrated or overcome by additional electrostatic force. Here, in the present case, Na^+ and Ca^{2+} chiefly feel a strong push from $\text{O}^{-1/2}$ as $g_{\text{Na},\text{Na}}$ gets larger (because $a_{\text{O}^{-1/2}}$ is large and $\text{O}^{-1/2}$ is kept inside the filter) as well as the electrostatic attractive force from $\text{O}^{-1/2}$. This can be clearly seen in Fig. 4. Note $4\times$ scaling of $[\text{O}^{-1/2}]$ concentration. In Fig. 4(a), $g_{\text{Na},\text{Na}} = 0$, concentration profiles of $\text{O}^{-1/2}$, Na^+ , and Ca^{2+} reach equilibrium (at the minimum of total energy) simply by diffusion and electrostatic force because the extra restraining force is felt by glutamate $\text{O}^{-1/2}$ only. $\text{O}^{-1/2}$, Na^+ , Ca^{2+} all form single-peak concentration profiles in the same region of the channel, the same range of z . Physically, Na^+ and Ca^{2+} are attracted to the focused $\text{O}^{-1/2}$ by electrostatic force. The attraction for Ca^{2+} has larger effect than the attraction for Na^+ because Ca^{2+} is divalent. Also, Na^+ and Ca^{2+} at the same time repel each other by electrostatic (and steric) forces.

This complex balance of forces can produce a wide range of behavior that varies a great deal as concentrations and conditions are changed. The biological function of channels and transporters has been defined experimentally for many decades by their behavior in complex ionic mixtures of variable composition, as different voltages are applied across the cell membrane. We have not yet investigated the properties of our model as concentrations of ions are made unequal on either side of the channel, as electrical potential is varied, or most importantly as different species of ions are included in ionic mixtures on both sides of the channel.

The interaction forces (without the attractive component) may be responsible for many of the single file properties of channels. More complete descriptions of Lennard Jones forces include an attractive component. The interaction forces with the attractive component might (conceivably) produce the phenomena that define transporters, whether they are co-transporters or counter transporters.

- (2) As $g_{\text{Na},\text{Na}}$ becomes larger in Fig. 4(b-f), the primary force is still the electrostatic attraction of Na^+ and Ca^{2+} by $\text{O}^{-1/2}$ but modified by finite-size effect (hard-sphere force). This electrostatic force will make peak(s) of Na^+ and Ca^{2+} occur in the ‘selectivity filter’ i.e., in the same region of the channel which contains the side chains $\text{O}^{-1/2}$. For Na^+ , Ca^{2+} , and $\text{O}^{-1/2}$, the hard-sphere forces between ions of the same species will make the concentration profiles flatter as $g_{\text{Na},\text{Na}}$ gets larger, when particles feel push from alike particles. Flattening is clearly seen in Fig. 4(b-f).
- (3) As $g_{\text{Na},\text{Na}}$ gets larger in Fig. 4(b-f), Ca^{2+} pushes Na^+ away from the middle part of filter and

forms a depletion zone and double-peak profile for Na^+ in Fig. 4(c-e). Depletion zones of this sort have profound effects on the selectivity of ion channels in Monte Carlo simulations, see Fig. 6 of reference⁹⁹ and ⁵⁴. Depletion zones have profound effects on the behavior of transistors^{132-135,162} and the selectivity of channels^{9,54,99}. A single transistor can have qualitatively distinct properties (e.g., gain, switch, logarithm, exponential) for different boundary electrical potentials ('bias' for one transistor; 'power supply' more generally) because the different boundary potentials produce different arrangement ('layering') of depletion zones. ***Each arrangement of layers or depletion zones makes the same transistor a different device, with a different device equation, corresponding to a different reduced model for the transistor. Different reduced models are appropriate for different conditions and have different functions.*** The function of the depletion zones found here is not yet known, nor is the pattern or effect of cycling through structures known, but the complex properties of the Ca/Na exchanger, wonderfully characterized by Hilgemann,¹⁶³⁻¹⁶⁶ immediately come to mind.

The major mechanism in Fig. 4(c-e) is still that Ca^{2+} is more attracted to $\text{O}^{-1/2}$ than Na^+ . However, with extra help from the inter-species hard-sphere force between Na^+ and Ca^{2+} (in addition to the electrical repulsive force between Na^+ and Ca^{2+}), Ca^{2+} is able to push Na^+ out of filter. Note that again Fig. 4(f) is an exception because all concentration profiles in it are very flat. In Fig. 4(f), the inter-species repulsive forces are greatly reduced and Na^+ resides in the middle of filter along with Ca^{2+} . Note that Ca^{2+} forms a single-peak concentration profile in all these cases, without splitting into two peaks. Na^+ , however, can form a double peak when $g_{\text{Na},\text{Na}}$ increases. The splitting occurs when the electrostatic attraction by $\text{O}^{-1/2}$ is large enough to survive the push of different-species from $\text{O}^{-1/2}$ and Na^+ in addition to the repulsive electrostatic force from Na^+ .

The singular behavior in Fig. 4(f) may have direct functional significance. Splitting of a single peak into a double peak can create a depletion zone that can dominate channel behavior (even though it is very small) because it is 'in series' with the rest of the channel. A depletion zone can block flow and create switching behavior as it does in transistors.

The depletion zones could help create the many 'states' of a channel, identified as activated, inactivated, slow inactivated, blocked, etc.² The depletion zones could be responsible for many of the similar (but correlated states) identified in classical experiments on transporters. In our calculations, of course, states arise as outputs of a self-consistent calculation and as a result of theory and computation, not as handcrafted metaphors summarizing the experimental experience and perspectives of structural biology and classical channology.²

Despite our enthusiasm and focus on our work, it must be clearly understood that our treatment of correlations is incomplete. We leave out many of the correlation effects of more complete variational treatments^{1,75,76} and the more subtle correlations in the BBGKY hierarchy,

derived for nonequilibrium systems²⁶⁸ like PNP (without finite size ions) from a Langevin description of trajectories in references^{167,168}. Our treatment is mathematically fully self-consistent but physically incomplete in its treatment of correlations and of course chemical interactions as well. The classical discussion of the BBGKY hierarchy and its treatment of correlations is not directly applicable to our analysis, however. The correlation forces of the hierarchy appear as driving forces in our partial differential equations and so the results of those forces are spread through all the terms of the solution of our partial differential equations. Thus, the effects of the correlations are likely to be more widespread than the effects in classical equilibrium analysis. Only detailed fitting of theory to data will show what correlations must be included in our model to explain which experimental data. Conclusions from equilibrium analysis may not apply.

- (4) From Table 1, Ca^{2+} binding ratio starts from 0.60214 when the finite size effect is zero, i.e., $g_{\text{Na},\text{Na}} = 0$. Affinity for Ca^{2+} in the filter region shows itself, even without the finite-size effect. This is obviously because Ca^{2+} feels a stronger electrostatic force than Na^+ because of the larger valence. The valence effect dominates even though the concentration of Ca^{2+} is much lower than that of Na^+ in reservoirs. The fact that valence effects overwhelm concentration effects when studying divalents has been known for at least one hundred years. The binding ratio of Ca^{2+} decreases, increases, and then decreases again as $g_{\text{Na},\text{Na}}$ increases, which shows the influence of the finite-size effect. The Ca^{2+} binding ratio roughly reaches its maximum at $g_{\text{Na},\text{Na}} = 0.01$ with the value 0.861. This is far larger than the 0.602 that occurs when the finite size effect is zero and helps generate the affinity of Ca (selectivity). These effects can be further seen from computational results shown later, when $g_{\text{Na},\text{Na}} = 0.01$.

We have not yet studied the effects of gradients of concentration. Note that in biological systems, gradients of Ca^{2+} are large and have profound effects in experiments. Calcium concentrations outside cells are typically $\sim 2 \times 10^{-3}\text{M}$, while those inside cells (cytoplasm) are $< 10^{-7}\text{M}$. There are many compartments within cells (vesicles, mitochondria, endoplasmic reticulum, sarcoplasmic reticulum) essential to living function that maintain distinctive concentrations of Ca^{2+} ***without which they cannot function***. We anticipate complex behavior of concentration profiles of ions within the selectivity filter when our model is studied in realistic ionic mixtures. It seems unlikely that these are uninvolved in biological function, however obscure that involvement seems today, and however difficult it is to discover. It seems wise to do calculations in conditions in which the systems can actually perform their natural function, and unwise to simulate conditions in which biological systems are known not to function properly.

Ca binding curve. In these calculations, we first studied how finite size effects changes the Ca binding curve, and the results are shown in Table 2 and its associated Fig. 5. We choose $g_{\text{Na},\text{Na}} = 0$ and an appropriate finite size effect by choosing $g_{\text{Na},\text{Na}} = 0.01$ to calculate the binding curves of Na^+ and Ca^{2+}

respectively. $V_{\max} = 200$ mV as above and boundary conditions $\phi_L = \phi_R = 100$ mV, and concentration of Na^+ inside and outside = 100 mM.

The results are shown in Table 2 and its associated Fig. 5. The finite-size effect enhances selectivity very much as observed previously in Monte Carlo simulations. The concentration profiles for different species is shown for both cases are shown in Figs. 6 and 7 respectively. Note $2\times$ scaling of $[\text{O}^{-1/2}]$ concentration in both figures. Fig. 6 shows that the increase of Ca^{2+} and decrease of Na^+ as Ca^{2+} concentration increases (in the baths on both sides of the channel). Increases are totally due to the interplay of diffusion and electrostatic force. There are no special chemical forces in our calculations. Binding forces are the output of our calculation, not inputs as in so many treatments of selectivity.

In our model, Na^+ and Ca^{2+} are both attracted to the confined $\text{O}^{-1/2}$. They repel each other at the same time. Na^+ and Ca^{2+} both form only single-peak concentration profiles, and therefore depletion of Na^+ in the middle of filter only occurs at the largest as Ca^{2+} concentration increases (on both sides).

Fig. 7 shows the extra influence of finite-size effect compared with Fig. 6. The single-peak profile of Ca^{2+} found in all cases means the pull from $\text{O}^{-1/2}$ by electrostatics survives the electrostatic repulsive force from Na^+ as well as the hard-sphere pushes from both $\text{O}^{-1/2}$ and Na^+ . The pull is so strong that there is no splitting and no double-peak profile.

However, the electrostatic pull for Na^+ from $\text{O}^{-1/2}$ is much smaller than its counterpart for Ca^{2+} . The combination of the hard-sphere pushes from both $\text{O}^{-1/2}$ and Ca^{2+} and also the electrostatic repulsive force from Ca^{2+} has qualitative effects. The concentration profile of Na^+ changes from a single-peak profile to a double-peak, as Ca^{2+} concentration increases (on both sides of the channel). Also, a depletion zone of Na^+ inside the filter is observed as Ca^{2+} concentration increases (on both sides of the channel). A depletion zone—as arises when a peak splits in two—can have profound functional consequences, because it is ‘in series’ with the entire channel. A series barrier can entirely block current flow.

DEEA Ca^{2+} binding curve. We have also computed the Ca^{2+} binding curve of a mutant sodium channel (DEEA) with 3 glutamate side chains. These are represented as 6 $\text{O}^{-1/2}$ particles, free moving inside the filter as in previous work, mostly Monte Carlo simulations previously cited. Fig. 8 shows the effect of a $-4e$ side chain in EEEE and a $-3e$ side chain in DEEA on the Ca^{2+} binding curve. Obviously, EEEE with a $-4e$ side chain has slightly larger affinity of Ca^{2+} than DEEA with $-3e$ side chain. This DEEA binding curve, employing the PNP-steric model, agrees well with its counterpart in⁷⁵ using the PNP-LJ model and in⁹⁹ using Monte Carlo simulations.

DEKA Ca^{2+} binding curve. Here we compute the Ca^{2+} binding curve of sodium channel (DEKA) with two glutamate side chains (4 $\text{O}^{-1/2}$ particles) and one lysine side chain (one NH_4^+ particle) free to move inside the filter. The Ca^{2+} binding curve is shown in Fig. 9, and the associated species concentration profiles are shown in Fig. 10. Note the scaling of $[\text{O}^{-1/2}]$ is the same as the scaling of other

concentrations in Fig. 10, unlike Fig. 4, Fig. 6 and Fig. 7. The loss in affinity with Ca^{2+} is obviously due to the existence of lysine side chain with +1e charge, though the net charge of glutamate and lysine side chains taken together is still $-1e$. We also computed an artificial EAAA channel with only one glutamate side chain ($2 \text{ O}^{-1/2}$ particles), in which the net permanent charge in the filter is $-1e$, to correspond precisely to the experimental situation, as discussed in⁹⁹ and references cited there. EAAA still has much higher affinity to Ca^{2+} than Na^+ (data not shown). The DEKA binding curve, employing the PNP-steric model, agrees well with its counterpart in⁷⁵ computed using the PNP-LJ model and also with its counterpart in⁹⁹ computed using Monte Carlo simulation. The concentration profiles of individual species shown in Fig. 10 also resemble those in⁹⁹. We have not yet performed the calculations with multiple ion species needed to evaluate the selectivity of the DEKA model to K^+ ions.

Discussion

Ion channel function depends on the properties of ionic solutions and ions in channels, along with the properties of the channel protein itself, and so it is necessary to relate our work to previous work in each field, emphasizing the properties of ions in bulk solutions, ions in proteins, and proteins that determine biological function in our models of channels, if not in the real world.

Relation to classical work on ionic solutions, Poisson Boltzmann and PNP. The limitations of Poisson Boltzmann and PNP models of ionic solutions have been known a very long time to the physical chemistry community but seem not to be so well known to either applied mathematicians or biophysicists. Exhaustive references to the literature are in^{52,59,65,169-171}. Applied mathematicians understandably are attracted to the simplicity of the Poisson Boltzmann/PNP equations and view them as a starting point for more realistic treatments.⁷⁰ Biophysicists² use the ‘independence principle’ that worked so well^{172,173} **when applied to membranes** in which ions flow through separated and independent protein channels.¹⁷⁴⁻¹⁷⁷ When channels that are not selective^{178,179} or two types of ions flow through one channel, as in classical ligand gated acetylcholine channels nAChRs,¹⁸⁰ the independence does not apply.

The independence principle is a restatement of Kohlraush’s ‘law’ of a century ago, that does *not* apply to bulk ionic solutions of the type found in biology (see eq. 3.27a,b on p. 125 of⁶⁷) References to the physical chemistry literature include^{21,57-63,66-69,74,129,158,169,171,181-230}. Many of these papers are strictly experimental, presenting compilations of physical chemistry data. These papers also show that ionic solutions are not well described by Poisson Boltzmann or PNP, if they contain divalents, multivalents, or mixtures of monovalents. (All biological solutions²³¹ are mixtures mostly involving divalents.) Interactions are strong in all ionic solutions, because they all satisfy global electroneutrality. Thus, ionic solutions are nothing like ideal, so the law of mass action (for example) does not apply as usually used

with rate constants independent of concentration. Note that rate constants in complex models will depend on each other as well as on concentration, because the electric field in one part of a channel (described by one rate constant) will interact with charges in another part of the channel (described by another rate constant). It is that variation of the electric field that allows Kirchoff's current law (and its generalization the Maxwell equations²³²⁻²³⁴) to be true. The electric field is long range and cannot be broken into independent spatial components as it is in most classical treatments.²

Classical work on channel proteins: permeation. Currents permeate biological membranes by flow through channel proteins that are either open or closed. A single ionic channel controls current by opening and closing (spontaneous 'gating'),^{5,6,235-237} thereby making a random telegraph signal²³⁸ studied in enormous detail for many (hundreds or thousands) of channel types^{178,179,239,240} using the wonderful techniques of single channel recording, patch clamp,^{6,241-245} or bilayer reconstitution.²⁴⁶

Sadly, the structures and mechanisms that produce this gating are still mostly unknown. However, progress is at hand.²⁴⁷⁻²⁵¹ Special structures modulate spontaneous stochastic gating in most channels to produce the macroscopic gating properties of classical electrophysiology.^{2,4,5,252,253} The properties of macroscopic modulated gating are complex, as is clear from the variety and number of complex schemes in the classic text², Ch. 18-19, e.g., Fig. 19.11. Some of these schemes involve nearly one hundred ill determined rate constants (Fig. 18-11 & Fig. 18-12 of ²) and have attracted the attention of literally hundreds of investigators over many decades.^{239,240} So far, no theoretical model can explain gating and selectivity using the fundamental physics that is described (crudely) in the PNP equations, but this situation may change.

Despite our ignorance of the mechanism of gating, the phenomena of spontaneous gating is remarkably clear, one might even say crystalline in clarity despite our amorphous structures involved. Once the single channel is open, the current through the single channel is remarkably stable. Single channel (mean) currents are independent of time from say 10 μ sec to 10 seconds or longer, strongly suggesting that the channel protein has only one structure over a range of (at least) 10^6 . A glance at an MD simulation of channels, or the numerical values of energies computed from Coulomb's law, or Lennard Jones potentials, suggests that the structure of the pore of the channel and the wall of the pore must be very constant indeed over these time scales. A change of radius of 3% would produce a change of current of at least (and probably much more than) 9%. Single channel currents are routinely resolved to within 2% (and can be resolved much better^{5,242,243,254-256} if necessary since stability is nearly perfect and signal to noise ratios are often larger than 50). The complexity and ignorance of gating mechanism reappears when we consider the time course of the opening and closing processes themselves (e.g., on a much faster time scale,²⁴⁴ or in cooled systems²⁴⁵). The opening and closing processes do not in fact have well defined time courses; and nothing seems to be known about their physical origin, in either case.

Classical work on channel proteins: permeation: selectivity. Once open, channels select between ions of different chemical type. Channels allow only some types of ions to flow, even though the different chemical types are quite similar. For example, Na^+ and K^+ ions differ only in diameter; Na^+ and Ca^{2+} ions differ only in charge. Simple models do surprisingly well in dealing with the selectivity of some types of channels. This work was reviewed in the Introduction of this paper and elsewhere.^{7,9,72}

Dealing with biological reality. It is important that the study of permeation and selectivity be made in the context of specific channels, using parameters known to properly fit a wide range of experimental data.^{9,16-18,90,94-97,99-112}

It is a surprise, particularly to structural biologists and traditional channologists, who customarily deal with metaphors²⁵⁷⁻²⁵⁹ and not quantitative fits to data, that powerful results, with quantitative fits to data in important cases, can arise from the Nonner & Eisenberg models with their very simple structure. We do not know why these models work, but one reason may be that the structures are the computed consequences of the forces in the model, so the structures of the channel protein and of the ionic solutions are always exactly self-consistent. Even tiny deviations the location of side chains from their free energy minimum produce large energetic and functional effects.^{54,93} ‘Exact’ self-consistency between channel protein and ionic solution seems to be necessary to make reasonable models. We suspect exact self-consistency is why some simulations fit some data so well.

If ‘exact’ self-consistency is necessary to make reasonable models, classical models in much of molecular biology²⁶⁰⁻²⁶⁴ will need to be reconsidered, even in much of chemistry,^{73,74} since classical chemical and biochemical models are almost never self-consistent. They almost never calculate the electric field from the charges present, let alone deal self-consistently with boundary conditions, steric forces or the resulting interactions of ‘everything’ with everything else. Our approach in this paper represents the ionic atmosphere around an ion consistently in a simplified way using the approximated LJ potential instead of the original LJ potential. Surely, we have not included all correlations among ions. Only detailed fitting to large amounts of data will show whether we have captured enough correlations, and captured them well enough.

It is also possible that the Nonner and Eisenberg models work well because the community of scientists working on them has recapitulated evolutionary history. Perhaps, those scientists have stumbled on the adaptation that biological organisms found eons ago, as evolution selected mutations that allowed cells to live and reproduce. It is even possible (for the same reason) that simple nearly one dimensional models will capture most of what we need to understand about time dependent nonequilibrium properties of channels.

Nonequilibrium treatments. An important advantage of the methods considered here is their extension to nonequilibrium in a mathematically precise and defined way, always fully self-consistent. Other approaches depend on physical approximations that are not self-consistent. They were the best that could

be done at the time, but cannot substitute for self-consistent treatments, in our view. For example, the DFT-PNP method^{18,105,107,108,110-112} is not self-consistent (i.e., does not precisely satisfy ‘sum rules’ of statistical mechanics^{265,266} or Poisson’s equation and boundary conditions), and apparently leaves out, relaxation and dielectrophoresis terms of the (more or less) self-consistent Debye-Hückel-Onsager equation. See the classical work²⁶⁷⁻²⁷⁸ and the textbook²⁰⁷ (p. 282 Fig. 7.7). DFT-PNP indeed assumes local equilibrium, as do other approaches using combinations of simulation and PNP equations²⁷⁹⁻²⁸¹, although it computes global flux.

It must be clearly understood that any assumption of local equilibrium is also an assumption of local zero flux. It is not clear how a system can have zero local flux and long range substantial flux, as does DFT-PNP, particularly when the system is a nanovalve connected in series with a high impedance entry process, and macroscopic baths. DFT-PNP is inconsistent in both its treatment of flux and electrostatics. Adopting models that are inherently inconsistent is dangerous because the results of calculations can depend on how the inconsistency is resolved and that resolution may be presented *sotto voce*, or chosen without conscious thought.

It is striking that highly successful PNP calculations in a closely related field—computational electronics—do not use inconsistent assumptions (like local equilibrium and global nonequilibrium) and always satisfy Poisson and boundary conditions with great accuracy. Simulations in computational electronics directly solve the relevant equations and so are fully self-consistent. Otherwise, they have difficulty accounting for the function of semiconductor devices that arise from small differences of large forces. Calculations of computational electronics account for macroscopic function using atomic scale models.^{8,9,11,12,134,136,149,282-284} Most treatments of ions in water and channels have been much less successful, perhaps because they are inconsistent.

Resolving inconsistencies can be a difficult task. It took a detailed stochastic analysis (lasting many years) of a second order Langevin equation with doubly conditioned non-differentiable Brownian trajectories^{285,286}, to resolve a similar inconsistency in an analysis of noninteracting particles. And the results of that analysis were not at all what had been anticipated, although they were pleasingly simple, when interpreted correctly with the classical theory of mass action.⁷⁴ The stochastic analysis allowed one to derive the law of mass action, but with variable rate constants that were specific functions of ‘everything’ in the system, as given by the analysis. It is not clear how one can evaluate or resolve the paradox of local equilibrium and global flow in DFT-PNP.

Flows in complex mixtures. An important advantage of the methods presented here is their indifference to flow. The methods work at thermodynamic equilibrium, and when flows are vigorous. Thus calculations can be done in the nonequilibrium situations and mixed ionic solutions used nearly always in experimental work. Such calculations require some further numerical work, because they involve many species of ions and of ionic tracers (radioactive ions with properties identical to non-radioactive

isotopes but present in trace amounts) that must be included appropriately in our Euler Lagrange equations. Such calculations will allow the direct simulation of the experiments used historically to define ‘single filing’ by ratios of unidirectional fluxes (e.g., which are estimated by net fluxes of tracers), and most importantly to define the properties of transporters of every type, whether they transport species in the same direction, or in opposite directions, or in both. It is likely that some of the properties attributed to interactions of ions with the channel protein actually occur between ions themselves.^{73,74} After all, interactions between ions had been ignored almost entirely in classical theories, because ions were treated as ideal solutions^{264,287,288} even when present at enormous concentrations.^{9,260} The effect of nonideality on the very definition of transporters remains to be investigated. This investigation can be done abstractly in general, but much better it can be done by realistic simulations of actual experimental setups using the steric PNP model and other models that deal even more realistically with interactions.

Future work: inverse problems. The distribution of permanent charge within the channel can be determined reliably from measurements of current voltage relations. Surprisingly, the inverse problem to determine the charge within the channel of the Nonner and Eisenberg model has been solved.¹⁶⁻¹⁸ The sensitivity to noise and errors is small when the problem is solved by standard methods of inverse problems. The inverse problem of interest to biologists has a well posed solution and can be used to determine the internal structure of the model channel, from the kind of experimental information recorded in hundreds if not thousands of laboratories every day. The inverse problem for steric PNP model needs to be studied so that experiments can be designed to reveal properties of interest.

Future work: one dimensional models. The forward PNP problem has in some ways been more difficult to compute than the inverse problem because it has had to deal with the complex geometry of the channel protein. The inverse problem hides much of this geometrical complexity in effective one dimensional parameters. In fact, most numerical work assumes simple geometry for the ion channel and reduces the problem to one dimension. These papers all assumed the pore diameter had some simple dependence on location, either parabolic or some kind of funnel shape that is easier to deal with analytically.^{24,25,47,48,51,88,116,143,147,148,167,289,290} Though some two dimensional and three dimensional work has been reported,^{24,35-40,43-45,49,50,281,291-295} many results have not been as well converged as one might wish, and others simply were not checked as carefully as references^{26,43,230} showed was necessary, as the semiconductor community had learned earlier (reviewed in¹³⁶, see¹⁴⁹). Very few computations have been reported using the real shape of channels and even then the accuracy of the electrostatic treatment was not sufficient to be sure that important details were resolved (Claudio Berti, personal communication^{139,296}). Obviously, the difficulty is expected to be much more when extending the traditional PNP equations to the modified ones of Eisenberg, *et al.*, and others.^{26,75-77,230}

The difficulties in deal with the full structural complexity of an ion channel should not be underestimated. The spatial resolution needed can put severe burdens on the memory bandwidth of even

modern day computers. The relation of structures determined by x-ray analysis of crystals to the spatial distribution of mass density of each species, spatial distribution of (effective) diffusion coefficient (of each species) and the spatial distribution of polarization (i.e., induced dielectric) charge cannot be determined by presently available methods. But these distributions must be specified with precision in three dimensional calculations. The issues of temporal properties are hardly ever discussed, yet the polarization properties of electrolyte solutions change tremendously in the time range from biological function to atomic motion. It is not clear how these effects are involved in protein function or how to include them in models. It may be that these issues are less important in one dimensional models than in three dimensional models because the lower dimensional models smooth over them in an appropriate way.

Time Dependence: future work. Future work needs to study each of the time dependent phenomena to see what part of the classical properties of ion channels, studied in innumerable experimental papers, might arise from a model as simple as that used here. Obviously, many of those classical properties will involve conformation changes of the channel protein not described by our simple model. But just as obviously, those conformation changes will be coupled to ions in the channel, by the electric field, and probably by steric interactions as well, and so everything must be analyzed together, ions, channel conformation, bathing solutions, ion flux, and current flow, as is usually the case in complex fluids flowing through complex spatial domains. Theory and simulations must allow everything to interact with everything else. They must not assume nothing interacts with nothing, as in ideal solutions.

Conclusions

Traditional PNP equations do not include the finite-size effect which is known to be significant in ionic solutions containing divalents, containing mixtures, and even in pure monovalent solutions more concentrated than say 50 mM. The concentration of ions in sea water, in and around cells, and inside channels is much higher than that. Therefore, classical PNP cannot describe the specific ion properties of bulk solutions like sea water and the solutions in living systems, the plasmas of life. It cannot predict the ion selectivity behavior of ion channels correctly. Here, we introduce the finite-size effect by treating ions and side chain as solid spheres and using hard sphere potentials to characterize this effect. Our work shows that selectivity is found in a simple one dimensional analysis and simulations.

Complex effects of changes in repulsion parameters shows a variety of states and depletion zones which are likely to be important in the functioning of channels and transporters. For example, the sudden appearance of a depletion zone, because of instability or stochastic fluctuation would surely gate a channel closed. If that gating happened on one side of a channel, the properties on the other side would be surely affected. 'Everything interacts with everything else' in these systems profoundly coupled by

Coulomb and steric exclusion forces. If an exclusion zone moved from one side of a channel to another, and then back and forth, the channel protein could easily produce a reciprocating ping pong effect and mimic the alternating access ‘states’ of transporters discovered with such wisdom and work by experimentalists who did not have the help of self-consistent models. The ‘everything interacts with everything’ nature of the crowded charge environment inside a channel—or active sites^{2,260,297}—makes such nonlinear interactions possible. It is not clear if the correlations included in our model are sufficient to produce ping pong effects or not: our model leaves out many forms of correlation, we are sad to say. It also remains to be seen whether biology actually uses such interactions at all. Alternating access could be produced in quite different ways, as most assume.

It is very important for the reader from the physical sciences to understand that complex systems of states and rates have been used by experimental biologists to characterize the function of the hundreds of channels^{178,179,239,240} and transporters²⁹⁸ studied by thousands of laboratories daily, because of their medical and biological importance.

It is very important for the reader from the biological sciences to understand that an enormous wealth of living behavior could be controlled by the physical phenomena described here, as outputs of a self-consistent model, as solutions of a set of partial differential equations and boundary conditions, without invoking classical vaguely defined effects. Those classical effects are more vitalistic than vital in many cases, in our view.

Early workers in molecular biology of some reputation, including Nobelists²⁹⁹⁻³⁰¹, attributed the secret of life to allosteric interactions of chemical signals acting on proteins and then channels.² It is striking to the biologists among us that a self-consistent model of ions and side chains in channels produces strong interactions over large distances (i.e., more than 1 nm) without invoking the metaphors of vitalistic allostery. The calculations of a self-consistent variational theory of the energetics of complex fluids seems ready to replace the poetry of our ancestors.

Self-consistent theory is only useful because it can be evaluated with computers. Those computers in turn are only possible because of the successful treatment of complex physical interactions by self-consistent mathematics. It is amusing that physicists learned to use self-consistent mathematics to analyze (control, and build) complex interacting systems of holes and electrons³⁰²⁻³⁰⁴ during the same years that biologists used poetry to describe complex interacting systems of cations and anions.

Channels are nearly enzymes^{9,297} and it is possible that the interactions described by models of the sort described here for channels underlie the complex interactions of a wide range of proteins that produce the special properties of life. Certainly, a theoretical and computational approach to biology and its molecules must allow everything to interact with everything else, instead of assuming that everything is ideal, and nothing interacts with nothing.

Acknowledgement

This work would not have been possible without the previous investigations of Dr. YunKyong Hyon. We are most grateful for his generosity in sharing all details with us in innumerable communications and discussions. We thank Wolfgang Nonner, and the referees for most helpful suggestions that materially improved the manuscript.

This research was sponsored in part by the National Science Council of Taiwan under Grant No. NSC-100-2115-M-035-001 (Dr. Horng). Dr. Eisenberg is supported by the Bard Endowed Chair of Rush University. He is particularly grateful for the administrative work he was not asked to do.

Figures

Fig. 1

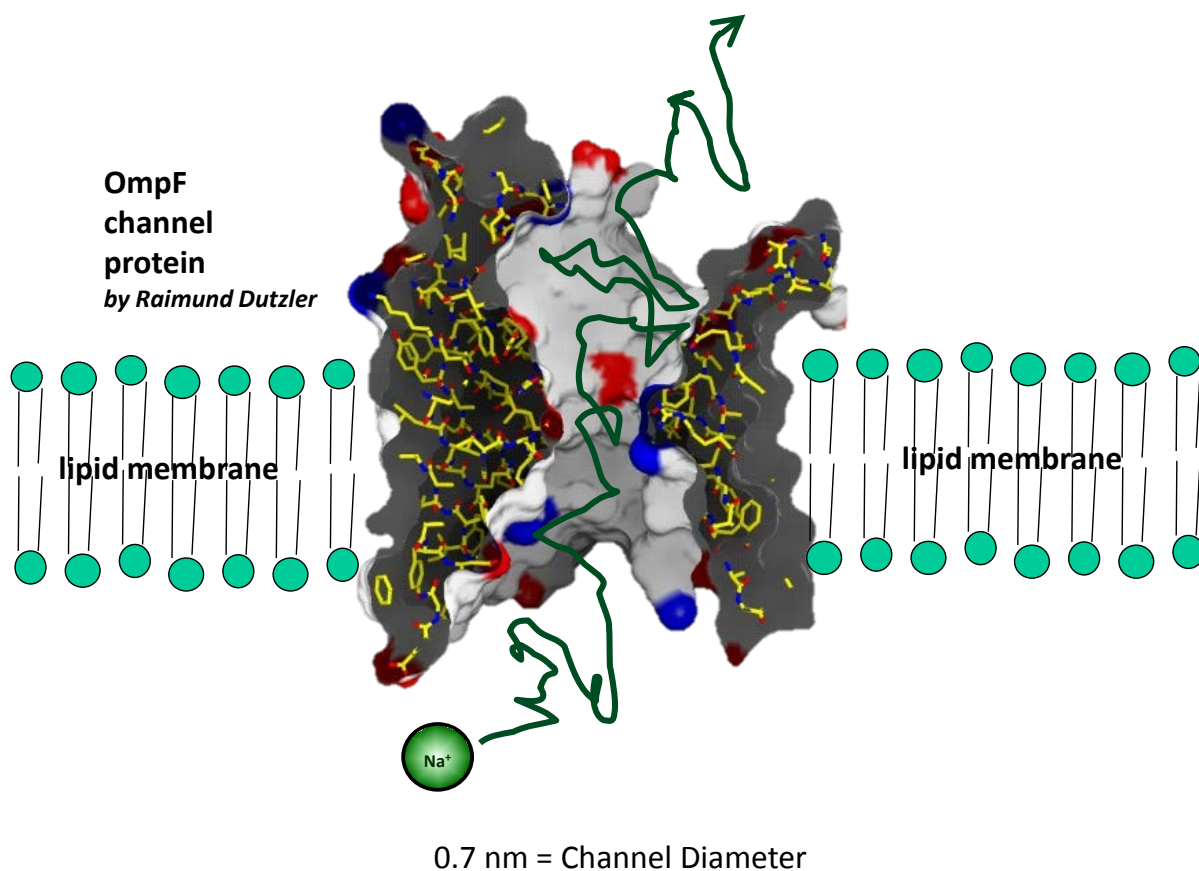


Figure 1. Typical geometry configuration of an ion channel. The usual time scale for an ion passing through the channel is ~ 200 nsec. Specifically, a channel passing 1 pA of current with an occupancy of 1 ion has a mean passage time of 160 nsec.

Fig. 2

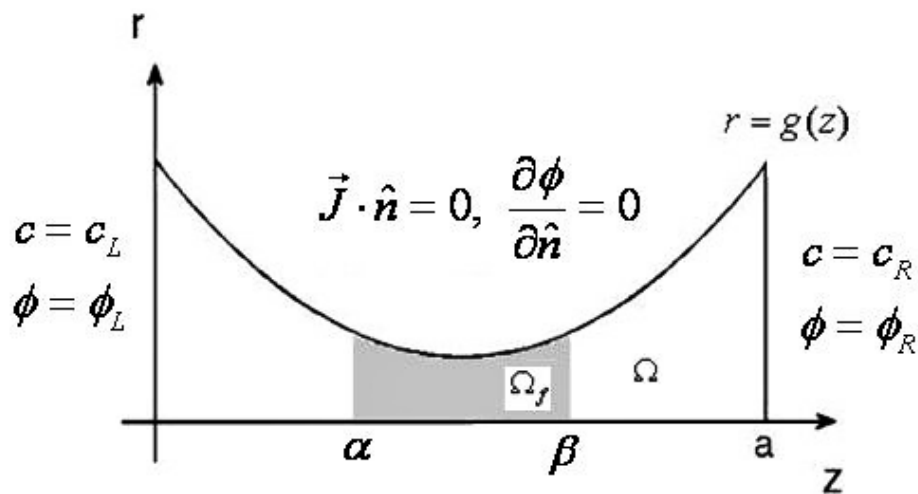
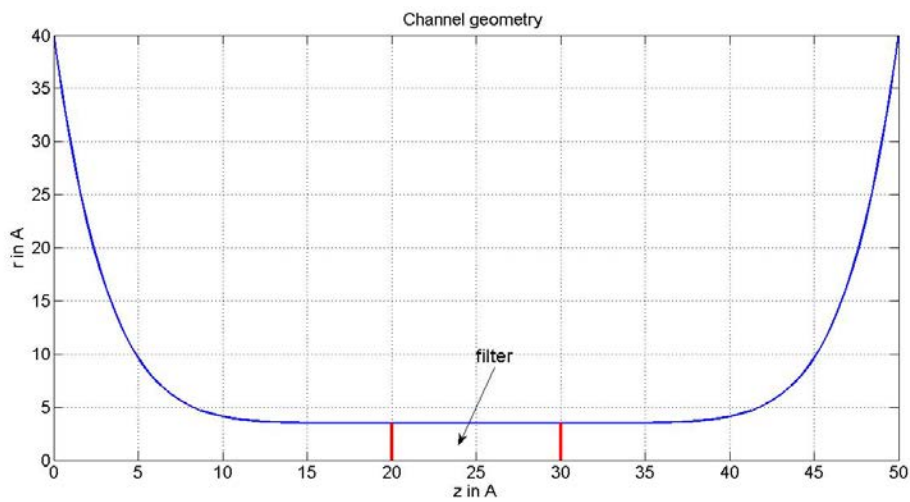


Figure 2. A cartoon of the configuration of ion channel with specified boundary conditions. Ω denotes the domain of whole channel; Ω_f denotes the filter part of the channel bounded by $\alpha \leq z \leq \beta$ and side wall; \hat{n} is the unit outward vector normal to side wall.

Fig. 3



]

Figure 3: Channel geometry. A precise specification of the geometry of our model.

Fig. 4

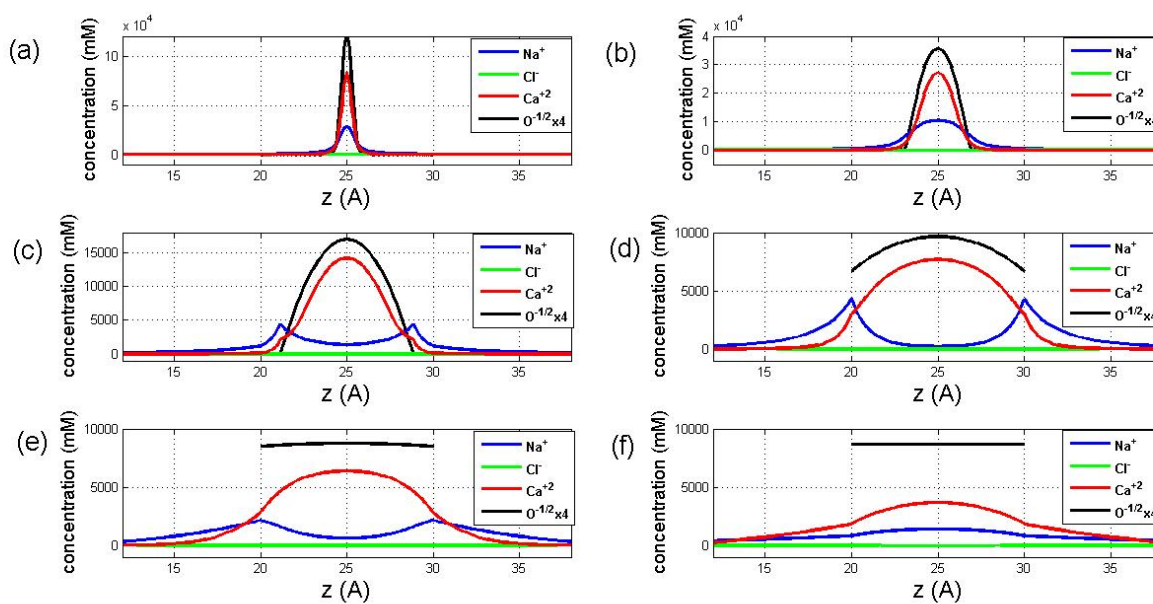


Figure 4: Species concentration distributions with various $g_{\text{Na},\text{Na}}$. With $V_{\text{max}} = 200$: (a) $g_{\text{Na},\text{Na}} = 0$; Ca^{2+} binding ratio=0.60214; (b) $g_{\text{Na},\text{Na}} = 10^{-4}$; Ca^{2+} binding ratio=0.59418; (c) $g_{\text{Na},\text{Na}} = 10^{-3}$; Ca^{2+} binding ratio=0.75433; (d) $g_{\text{Na},\text{Na}} = 10^{-2}$; Ca^{2+} binding ratio=0.86109; (e) $g_{\text{Na},\text{Na}} = 10^{-1}$; Ca^{2+} binding ratio=0.82580; (f) $g_{\text{Na},\text{Na}} = 1$; Ca^{2+} binding ratio=0.71644 and the symmetrical symmetric boundary conditions: $[\text{Ca}^{2+}]_L = [\text{Ca}^{2+}]_R = 1\text{mM}$, $[\text{Na}^+]_L = [\text{Na}^+]_R = 100\text{mM}$, $\phi_L = \phi_R = 100\text{mV}$. Note $4\times$ scaling of $[\text{O}^{-1/2}]$ concentration.

Fig. 5

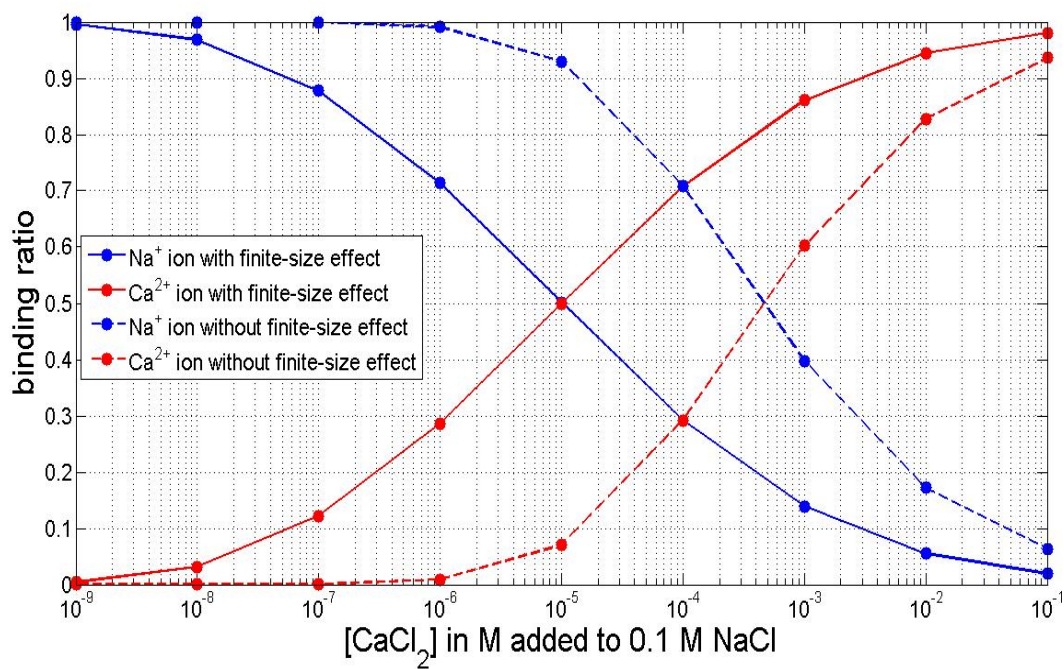


Figure 5: Binding curves corresponding to Table 2.

Fig. 6

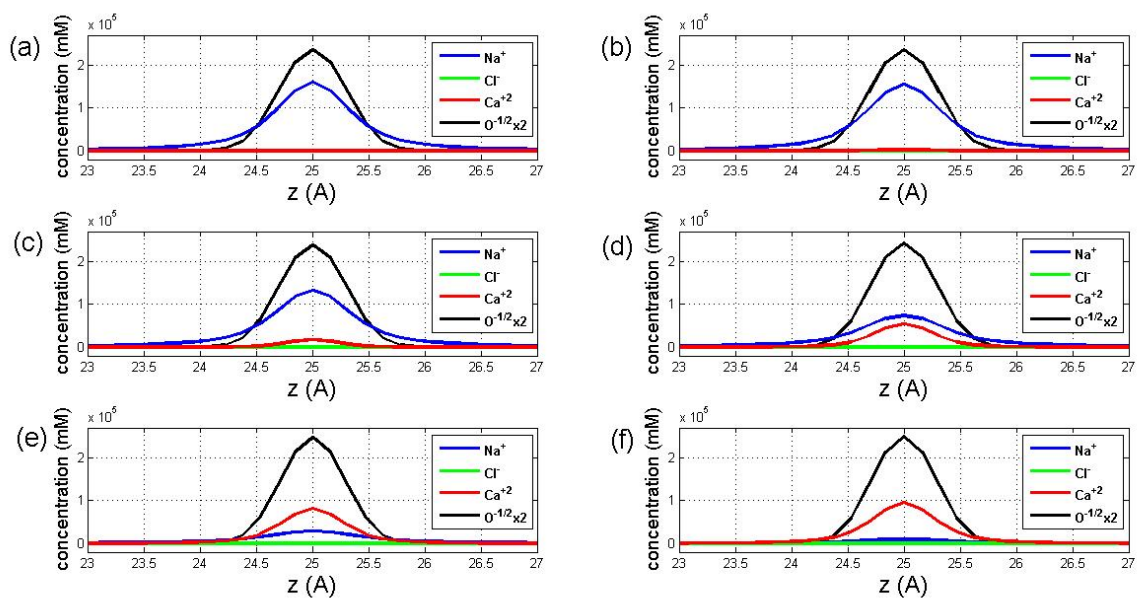


Figure 6: Species concentration distributions under various $[Ca^{2+}]_L = [Ca^{2+}]_R$ with $g_{Na,Na} = 0$ (no finite-size effect). $V_{\max} = 200$, $\phi_L = \phi_R = 100mV$, and $[Na^+]_L = [Na^+]_R = 100mM$:
 (a) $[Ca^{2+}]_L = [Ca^{2+}]_R = 10^{-7} M$; (b) $[Ca^{2+}]_L = [Ca^{2+}]_R = 10^{-6} M$; (c) $[Ca^{2+}]_L = [Ca^{2+}]_R = 10^{-5} M$;
 (d) $[Ca^{2+}]_L = [Ca^{2+}]_R = 10^{-4} M$; (e) $[Ca^{2+}]_L = [Ca^{2+}]_R = 1mM$; (f) $[Ca^{2+}]_L = [Ca^{2+}]_R = 10mM$. Note $2\times$ scaling of $[O^{-1/2}]$ concentration.

Fig. 7

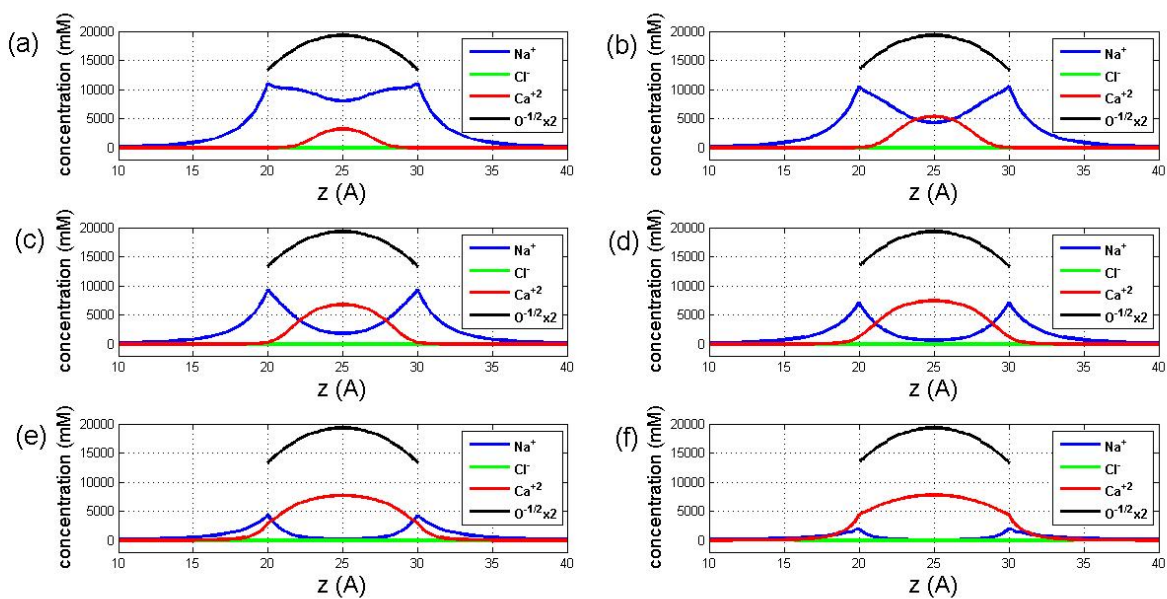


Figure 7: Species concentration distributions under various $[\text{Ca}^{2+}]_L = [\text{Ca}^{2+}]_R$ with $g_{\text{Na},\text{Na}} = 0.01$ (with finite-size effect). $V_{\text{max}} = 200$, $\phi_L = \phi_R = 100 \text{mV}$, and $[\text{Na}^+]_L = [\text{Na}^+]_R = 100 \text{mM}$:

(a) $[\text{Ca}^{2+}]_L = [\text{Ca}^{2+}]_R = 10^{-7} M$, (b) $[\text{Ca}^{2+}]_L = [\text{Ca}^{2+}]_R = 10^{-6} M$, (c) $[\text{Ca}^{2+}]_L = [\text{Ca}^{2+}]_R = 10^{-5} M$,

(d) $[\text{Ca}^{2+}]_L = [\text{Ca}^{2+}]_R = 10^{-4} M$, (e) $[\text{Ca}^{2+}]_L = [\text{Ca}^{2+}]_R = 1 \text{mM}$, (f) $[\text{Ca}^{2+}]_L = [\text{Ca}^{2+}]_R = 10 \text{mM}$. Note $2 \times$ scaling of $[\text{O}^{-1/2}]$ concentration.

Fig. 8

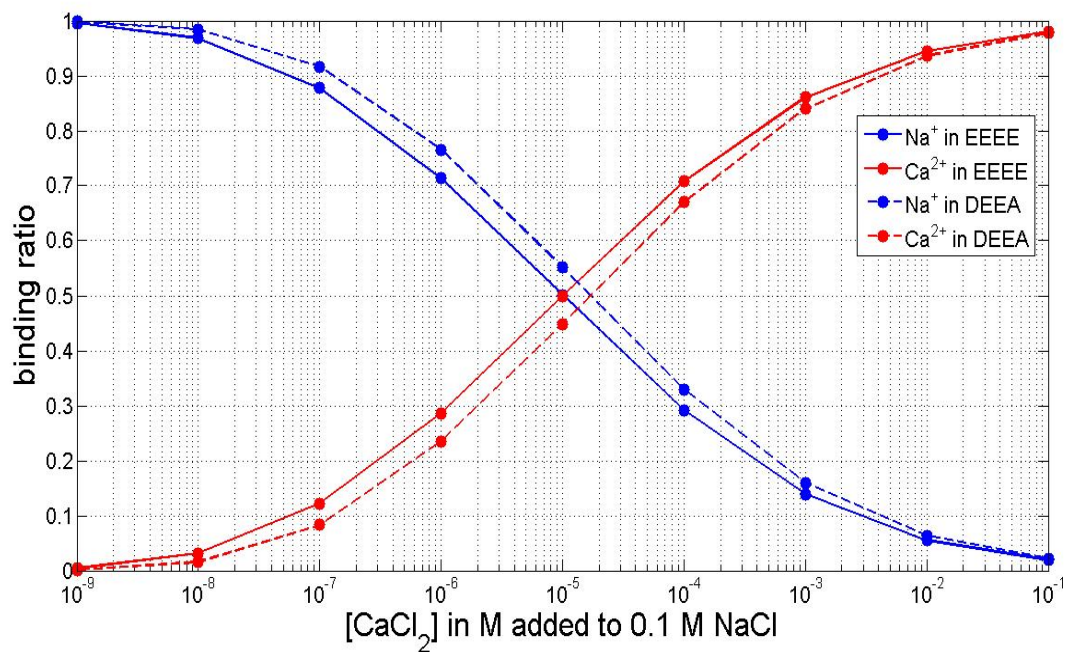


Figure 8: Binding curves of EEEE (-4e) and DEEA (-3e).

Fig. 9

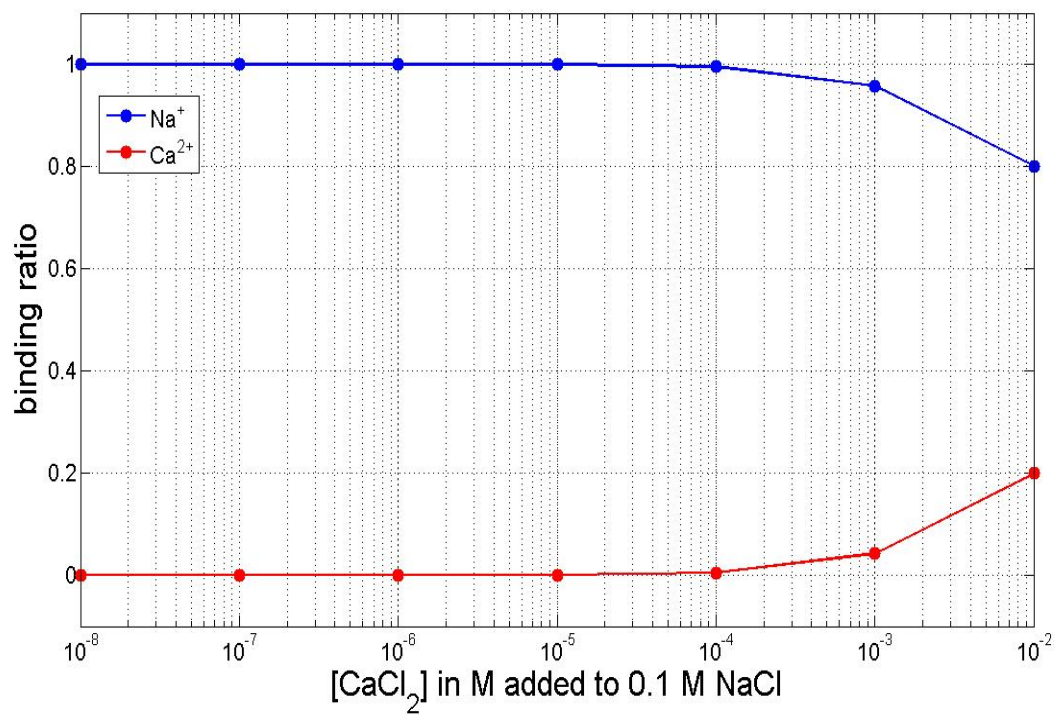


Figure 9: Binding curves of DEKA (-1e).

Fig. 10

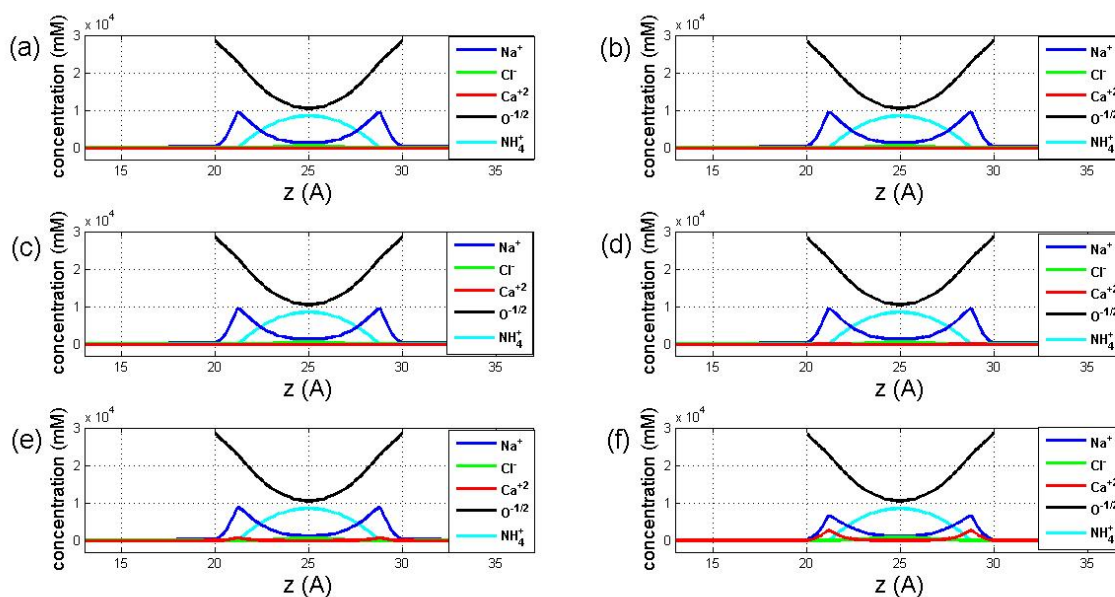


Figure 10: Species concentration distributions under various $[Ca^{+2}]_L = [Ca^{+2}]_R$ with $g_{Na,Na} = 0.01$ (having finite-size effect). $V_{\max} = -200$ for glutamate side chain, $V_{\max} = 200$ for lysine side chain, $\phi_L = \phi_R = 100mV$, and $[Na^+]_L = [Na^+]_R = 100mM$: (a) $[Ca^{2+}]_L = [Ca^{2+}]_R = 10^{-7} M$, (b) $[Ca^{2+}]_L = [Ca^{2+}]_R = 10^{-6} M$, (c) $[Ca^{2+}]_L = [Ca^{2+}]_R = 10^{-5} M$, (d) $[Ca^{2+}]_L = [Ca^{2+}]_R = 10^{-4} M$, (e) $[Ca^{2+}]_L = [Ca^{2+}]_R = 1mM$, (f) $[Ca^{2+}]_L = [Ca^{2+}]_R = 10mM$. Note the scaling of $[O^{-1/2}]$ is the same as the scaling of other concentrations in Fig. 10, unlike Fig. 4, Fig. 6 and Fig. 7.

Table 1: Effect of increasing ε_{global} on Ca binding ratio with $[Ca^{2+}]_L = [Ca^{2+}]_R = 1mM$
 $[Na^+]_L = [Na^+]_R = 100mM$, $\phi_L = \phi_R = 100mV$, $V_{max} = 200$.

$g_{Na,Na}$	0	10^{-4}	10^{-3}	10^{-2}	10^{-1}	1
$g_{Na,Cl}$	0	0	0	0	0	0
$g_{Cl,Cl}$	0	0	0	0	0	0
$g_{Na,Ca}$	0	6.41×10^{-5}	6.41×10^{-4}	6.41×10^{-3}	6.42×10^{-2}	6.42×10^{-1}
$g_{Cl,Ca}$	0	0	0	0	0	0
$g_{Ca,Ca}$	0	1.64×10^{-4}	1.64×10^{-3}	1.64×10^{-2}	1.64×10^{-1}	1.64
$g_{Na,O^{-1/2}}$	0	8.19×10^{-4}	8.19×10^{-3}	8.19×10^{-2}	8.20×10^{-1}	8.20
$g_{Cl,O^{-1/2}}$	0	0	0	0	0	0
$g_{Ca,O^{-1/2}}$	0	1.00×10^{-3}	1.00×10^{-2}	1.00×10^{-1}	1.0034	1.00×10^1
$g_{O^{-1/2},O^{-1/2}}$	0	1.63×10^{-2}	1.64×10^{-1}	1.64	1.65×10	1.64×10^2
Ca binding ratio	0.602	0.594	0.754	0.861	0.825	0.72

Table 2: Ca binding ratio vs. $[Ca^{2+}]_L = [Ca^{2+}]_R$ with $g_{Na,Na} = 0$ (no finite-size effect) and $g_{Na,Na} = 0.01$ (having finite-size effect). $V_{max} = 200$, $\phi_L = \phi_R = 100mV$, and $[Na^+]_L = [Na^+]_R = 100 mM$.

$[Ca^{+2}]$ in mM	Ca binding ratio $g_{Na,Na} = 0$	Ca binding ratio $g_{Na,Na} = 0.01$
10^{-6}	9.2286×10^{-6}	4.4525×10^{-3}
10^{-5}	9.2257×10^{-5}	3.1819×10^{-2}
10^{-4}	9.1970×10^{-4}	0.12233
10^{-3}	8.9241×10^{-3}	0.28671
10^{-2}	7.0641×10^{-2}	0.49926
10^{-1}	0.29171	0.70778
1	0.60214	0.86109
10	0.82816	0.94502
100	0.93661	0.98080

References

- (1) Lin, T. C.; Eisenberg, B. (*in preparation*) **2012**.
- (2) Hille, B. *Ionic Channels of Excitable Membranes*, 3rd ed.; Sinauer Associates Inc.: Sunderland, 2001.
- (3) Ashcroft, F. M. *Ion Channels and Disease*; Academic Press: New York, 1999.
- (4) Neher, E. Ion channels for communication between and within cells Nobel Lecture, December 9, 1991. In *Nobel Lectures, Physiology or Medicine 1991-1995*; Ringertz, N., Ed.; World Scientific Publishing Co: Singapore, 1997; pp 10.
- (5) Neher, E.; Sakmann, B. *Nature* **1976**, *260*, 799.
- (6) Sakmann, B.; Neher, E. *Single Channel Recording.*, Second ed.; Plenum: New York, 1995.
- (7) Eisenberg, B. **2012**, Available on arXiv as <http://arxiv.org/abs/1206.6490>.
- (8) Eisenberg, B. *Fluctuations and Noise Letters* **2012**, *11*, 76.
- (9) Eisenberg, B. Crowded Charges in Ion Channels. In *Advances in Chemical Physics*; John Wiley & Sons, Inc., 2011; pp 77.
- (10) Eisenberg, B. *The Journal of Physical Chemistry C* **2010**, *114*, 20719.
- (11) Eisenberg, R. S. Atomic Biology, Electrostatics and Ionic Channels. In *New Developments and Theoretical Studies of Proteins*; Elber, R., Ed.; World Scientific: Philadelphia, 1996; Vol. 7; pp 269.
- (12) Eisenberg, R. S. *J. Membrane Biol.* **1996**, *150*, 1.
- (13) Warshel, A. *Proc Natl Acad Sci U S A* **1978**, *75*, 5250.
- (14) Warshel, A.; Russell, S. T. *Quarterly Review of Biophysics* **1984**, *17*, 283.
- (15) Warshel, A.; Sharma, P. K.; Chu, Z. T.; Aqvist, J. *Biochemistry* **2007**, *46*, 1466.
- (16) Arning, K. Mathematical Modelling and Simulation of Ion Channels, Johannes Kepler University Linz, 2009.
- (17) Arning, K.; Burger, M.; Eisenberg, R. S.; Engl, H. W.; He, L. *PAMM* **2007**, *7*, 1120801.
- (18) Burger, M.; Eisenberg, R. S.; Engl, H. *SIAM J Applied Math* **2007**, *67*, 960.
- (19) Engl, H. W.; Hanke, M.; Neubauer, A. *Regularization of Inverse Problems* Kluwer: Dordrecht, The Netherlands, 2000.
- (20) Kaipio, J.; Somersalo, E. *Statistical and Computational Inverse Problems* Springer: New York, 2005.
- (21) Bazant, M. Z.; Thornton, K.; Ajdari, A. *Physical Review E* **2004**, *70*, 021506.
- (22) Coalson, R. D.; Kurnikova, M. G. *IEEE Trans Nanobioscience* **2005**, *4*, 81.
- (23) Eisenberg, R.; Chen, D. *Biophysical Journal* **1993**, *64*, A22.
- (24) Liu, W.; Wang, B. *J. Dynam. Differential Equations* **2010**, *22*, 413.
- (25) Singer, A.; Norbury, J. *SIAM J Appl Math* **2009**, *70*, 949.
- (26) Zheng, Q.; Wei, G.-W. *J Chem Phys* **2011**, *134*, 194101.
- (27) Chen, D. P.; Lear, J.; Eisenberg, R. S. *Biophys. J.* **1997**, *72*, 97.

- (28) Dieckmann, G. R.; Lear, J. D.; Zhong, Q.; Klein, M. L.; DeGrado, W. F.; Sharp, K. A. *Biophysical Journal* **1999**, *76*, 618.
- (29) Chen, D. P.; Nonner, W.; Eisenberg, R. S. *Biophys. J.* **1995**, *68*, A370.
- (30) Chen, D.; Xu, L.; Tripathy, A.; Meissner, G.; Eisenberg, R. *Biophys. J.* **1997**, *73*, 1337.
- (31) Allen, T. W.; Kuyucak, S.; Chung, S. H. *Biophys J* **1999**, *77*, 2502.
- (32) Chen, D.; Xu, L.; Tripathy, A.; Meissner, G.; Eisenberg, B. *Biophysical Journal* **1999**, *76*, 1346.
- (33) Corry, B.; Kuyucak, S.; Chung, S. H. *J Gen Physiol* **1999**, *114*, 597.
- (34) Eisenberg, R. S. *Journal of Membrane Biology* **1999**, *171*, 1.
- (35) Hollerbach, U.; Chen, D.; Nonner, W.; Eisenberg, B. *Biophysical Journal* **1999**, *76*, A205.
- (36) Kurnikova, M. G.; Coalson, R. D.; Graf, P.; Nitzan, A. *Biophysical Journal* **1999**, *76*, 642.
- (37) Corry, B.; Kuyucak, S.; Chung, S. H. *Biophys J* **2000**, *78*, 2364.
- (38) Graf, P.; Nitzan, A.; Kurnikova, M. G.; Coalson, R. D. *Journal of Physical Chemistry B* **2000**, *104*, 12324.
- (39) Hollerbach, U.; Chen, D. P.; Busath, D. D.; Eisenberg, B. *Langmuir* **2000**, *16*, 5509.
- (40) Moy, G.; Corry, B.; Kuyucak, S.; Chung, S. H. *Biophys J* **2000**, *78*, 2349.
- (41) Im, W.; Roux, B. *Biophysical Journal* **2001**, *115*, 4850.
- (42) Edwards, S.; Corry, B.; Kuyucak, S.; Chung, S. H. *Biophys J* **2002**, *83*, 1348.
- (43) Hollerbach, U.; Chen, D.-P.; Eisenberg, R. S. *Journal of Computational Science* **2002**, *16*, 373.
- (44) Hollerbach, U.; Eisenberg, R. *Langmuir* **2002**, *18*, 3262.
- (45) Im, W.; Roux, B. *Journal of Molecular Biology* **2002**, *322*, 851.
- (46) Im, W.; Roux, B. *Journal of Molecular Biology* **2002**, *319*, 1177.
- (47) van der Straaten, T. A.; Tang, J.; Eisenberg, R. S.; Ravaioli, U.; Aluru, N. R. *J. Computational Electronics* **2002**, *1*, 335.
- (48) van der Straaten, T. A.; Tang, J. M.; Eisenberg, R. S.; Ravaioli, U.; Aluru, N.; Varma, S.; E., J. *Biophys. J.* **2002**, *82*, 207a.
- (49) Corry, B.; Kuyucak, S.; Chung, S. H. *Biophys J* **2003**, *84*, 3594.
- (50) Mamonov, A. B.; Coalson, R. D.; Nitzan, A.; Kurnikova, M. G. *Biophys J* **2003**, *84*, 3646.
- (51) Nadler, B.; Hollerbach, U.; Eisenberg, R. S. *Phys Rev E Stat Nonlin Soft Matter Phys* **2003**, *68*, 021905.
- (52) Eisenberg, B. **2012**, Available on arXiv as <http://arxiv.org/abs/1207.4737> as arXiv 1207.4737
- (53) Eisenberg, B. *Biophysical Chemistry* **2003**, *100*, 507
- (54) Giri, J.; Fonseca, J. E.; Boda, D.; Henderson, D.; Eisenberg, B. *Phys Biol* **2011**, *8*, 026004.
- (55) Ganguly, P.; Mukherji, D.; Junghans, C.; van der Vegt, N. F. A. *Journal of Chemical Theory and Computation* **2012**, *8*, 1802.
- (56) Molina, J. J.; Dufreche, J.-F.; Salanne, M.; Bernard, O.; Turq, P. *J Chem Phys* **2011**, *135*, 234509.
- (57) Fraenkel, D. *The Journal of Physical Chemistry B* **2010**, *115*, 557.
- (58) Kunz, W.; Neueder, R. An Attempt at an Overview. In *Specific Ion Effects*; Kunz, W., Ed.; World

Scientific Singapore, 2009; pp 11.

- (59) Kunz, W. *Specific Ion Effects*; World Scientific Singapore, 2009.
- (60) Kontogeorgis, G. M.; Folas, G. K. *Thermodynamic Models for Industrial Applications: From Classical and Advanced Mixing Rules to Association Theories*; John Wiley & Sons, Ltd, 2009.
- (61) Abbas, Z.; Ahlberg, E.; Nordholm, S. *The Journal of Physical Chemistry B* **2009**, *113*, 5905.
- (62) Lee, L. L. *Molecular Thermodynamics of Electrolyte Solutions*; World Scientific Singapore, 2008.
- (63) Jungwirth, P.; Winter, B. *Annual Review of Physical Chemistry* **2008**, *59*, 343.
- (64) Jungwirth, P.; Finlayson-Pitts, B. J.; Tobias, D. J. *Chemical Reviews* **2006**, *106*, 1137.
- (65) Ben-Naim, A. *Molecular Theory of Solutions*; Oxford: New York, 2006; Vol. .
- (66) Fawcett, W. R. *Liquids, Solutions, and Interfaces: From Classical Macroscopic Descriptions to Modern Microscopic Details*; Oxford University Press: New York, 2004.
- (67) Barthel, J.; Krienke, H.; Kunz, W. *Physical Chemistry of Electrolyte Solutions: Modern Aspects*; Springer: New York, 1998.
- (68) Durand-Vidal, S.; Turq, P.; Bernard, O.; Treiner, C.; Blum, L. *Physica A* **1996**, *231*, 123.
- (69) Pitzer, K. S. *Thermodynamics*, 3rd ed.; McGraw Hill: New York, 1995.
- (70) Xu, Z.; Cai, W. *SIAM Review* **2011**, *53*, 683.
- (71) Chazalviel, J.-N. *Coulomb Screening by Mobile Charges*; Birkhäuser: New York, 1999.
- (72) Eisenberg, B. *Transactions of the Faraday Society* **2012**, (in the press: DOI:10.1039/C2FD20066J), available at <http://arxiv.org/abs/1206.1517> cite as 1206.1517v1.
- (73) Eisenberg, B. *Posted on arXiv.org with Paper ID arXiv:1105.0184v1* **2011**.
- (74) Eisenberg, B. *Chemical Physics Letters* **2011**, *511*, 1.
- (75) Eisenberg, B.; Hyon, Y.; Liu, C. *Journal of Chemical Physics* **2010**, *133*, 104104
- (76) Hyon, Y.; Eisenberg, B.; Liu, C. *Communications in Mathematical Sciences* **2011**, *9*, 459.
- (77) Mori, Y.; Liu, C.; Eisenberg, R. S. *Physica D: Nonlinear Phenomena* **2011**, *240*, 1835.
- (78) Hyon, Y.; Fonseca, J. E.; Eisenberg, B.; Liu, C. *Discrete and Continuous Dynamical Systems Series B (DCDS-B)* **2012**, *17*, 2725
- (79) Zhang, J.; Gong, X.; Liu, C.; Wen, W.; Sheng, P. *Physical Review Letters* **2008**, *101*, 194503.
- (80) Doi, M. *Journal of the Physical Society of Japan* **2009**, *78*, 052001.
- (81) Liu, C. An Introduction of Elastic Complex Fluids: An Energetic Variational Approach. In *Multi-scale Phenomena in Complex Fluids: Modeling, Analysis and Numerical Simulations*; Hou, T. Y., Liu, C., Liu, J.-g, Ed.; World Scientific Publishing Company: Singapore, 2009.
- (82) Lin, F.-H.; Liu, C.; Zhang, P. *Communications on Pure and Applied Mathematics* **2007**, *60*, 838.
- (83) Lin, F.-H.; Liu, C.; Zhang, P. *Communications on Pure and Applied Mathematics* **2005**, *58*, 1437.
- (84) Sheng, P.; Zhang, J.; Liu, C. *Progress of Theoretical Physics Supplement No. 175* **2008**, 131.
- (85) Larson, R. G. *The Structure and Rheology of Complex Fluids* Oxford: New York, 1995.
- (86) Buyukdagli, S.; Manghi, M.; Palmeri, J. *Physical Review E* **2010**, *81*, 041601.

- (87) Nonner, W.; Chen, D. P.; Eisenberg, B. *Biophysical Journal* **1998**, *74*, 2327.
- (88) Nonner, W.; Eisenberg, B. *Biophys. J.* **1998**, *75*, 1287.
- (89) Nonner, W.; Catacuzzeno, L.; Eisenberg, B. *Biophysical Journal* **2000**, *79*, 1976.
- (90) Boda, D.; Gillespie, D.; Nonner, W.; Henderson, D.; Eisenberg, B. *Phys Rev E Stat Nonlin Soft Matter Phys* **2004**, *69*, 046702.
- (91) Boda, D.; Busath, D.; Eisenberg, B.; Henderson, D.; Nonner, W. *Physical Chemistry Chemical Physics (PCCP)* **2002**, *4*, 5154.
- (92) Boda, D.; Henderson, D.; Busath, D. *Molecular Physics* **2002**, *100*, 2361.
- (93) Eisenberg, B. *Institute of Mathematics and its Applications* **2009**, IMA University of Minnesota <http://www.ima.umn.edu/2008>.
- (94) Boda, D.; Giri, J.; Henderson, D.; Eisenberg, B.; Gillespie, D. *J Chem Phys* **2011**, *134*, 055102.
- (95) Boda, D.; Valisko, M.; Henderson, D.; Eisenberg, B.; Gillespie, D.; Nonner, W. *J. Gen. Physiol.* **2009**, *133*, 497.
- (96) Boda, D.; Nonner, W.; Henderson, D.; Eisenberg, B.; Gillespie, D. *Biophys. J.* **2008**, *94*, 3486.
- (97) Krauss, D.; Eisenberg, B.; Gillespie, D. *European Biophysics Journal* **2011**, *40*, 775.
- (98) Dolphin, A. C. *British Journal of Pharmacology* **2006**, *147*, S56.
- (99) Boda, D.; Nonner, W.; Valisko, M.; Henderson, D.; Eisenberg, B.; Gillespie, D. *Biophys. J.* **2007**, *93*, 1960.
- (100) Miedema, H.; Meter-Arkema, A.; Wierenga, J.; Tang, J.; Eisenberg, B.; Nonner, W.; Hektor, H.; Gillespie, D.; Meijberg, W. *Biophys J* **2004**, *87*, 3137.
- (101) Miedema, H.; Vrouenraets, M.; Wierenga, J.; Gillespie, D.; Eisenberg, B.; Meijberg, W.; Nonner, W. *Biophys J* **2006**, *91*, 4392.
- (102) Vrouenraets, M.; Wierenga, J.; Meijberg, W.; Miedema, H. *Biophys J* **2006**, *90*, 1202.
- (103) Malasics, A.; Boda, D.; Valisko, M.; Henderson, D.; Gillespie, D. *Biochimica et Biophysica Acta* **2010**, *1798*, 2013.
- (104) Krauss, D.; Gillespie, D. *European Biophysics Journal* **2010**, *39*, 1513.
- (105) Gillespie, D.; Giri, J.; Fill, M. *Biophysical Journal* **2009**, *97*, pp. 2212
- (106) Gillespie, D.; Fill, M. *Biophys. J.* **2008**, *95*, 3706.
- (107) Gillespie, D.; Boda, D.; He, Y.; Apel, P.; Siwy, Z. S. *Biophys. J.* **2008**, *95*, 609.
- (108) Gillespie, D.; Boda, D. *Biophys. J.* **2008**, *95*, 2658.
- (109) Gillespie, D. *Biophys J* **2008**, *94*, 1169.
- (110) Gillespie, D.; Valisko, M.; Boda, D. *Journal of Physics: Condensed Matter* **2005**, *17*, 6609.
- (111) Gillespie, D.; Nonner, W.; Eisenberg, R. S. *Physical Review E* **2003**, *68*, 0313503.
- (112) Gillespie, D.; Nonner, W.; Eisenberg, R. S. *Journal of Physics (Condensed Matter)* **2002**, *14*, 12129.
- (113) Chen, D. P. Nonequilibrium thermodynamics of transports in ion channels. In *Progress of Cell Research: Towards Molecular Biophysics of Ion Channels*; Sokabe, M., Auerbach, A., Sigworth, F.,

Eds.; Elsevier: Amsterdam, 1997; pp 269.

- (114) Chen, D.; Xu, L.; Tripathy, A.; Meissner, G.; Eisenberg, R. *Biophys. J.* **1997**, *72*, A108.
- (115) Hyon, Y.; Kwak, D. Y.; Liu, C. *Discrete and Continuous Dynamical Systems (DCDS-A)* **2010**, *26*, 1291
- (116) Barcilon, V.; Chen, D. P.; Eisenberg, R. S. *SIAM J. Applied Math* **1992**, *52*, 1405.
- (117) Gillespie, D.; Eisenberg, R. S. *European Biophysics Journal* **2002**, *31*, 454.
- (118) Gillespie, D.; Nonner, W.; Eisenberg, R. S. *Biophysical Journal Abstract* **2002**, *84*, 67a.
- (119) Gardner, C. L.; Nonner, W.; Eisenberg, R. S. *Journal of Computational Electronics* **2004**, *3*, 25.
- (120) Aguilera-Arzo, M.; Aguilera, V.; Eisenberg, R. S. *European Biophysics Journal*, **2005**, *34*, 314.
- (121) Luchinsky, D. G.; Tindjong, R.; Kaufman, I.; McClintock, P. V. E.; Eisenberg, R. S. *Physical Review E (Statistical, Nonlinear, and Soft Matter Physics)* **2009**, *80*, 021925.
- (122) Doi, M. *Journal of Physics of Condensed Matter* **2011**, *23*, 284118.
- (123) Hou, T. Y.; Liu, C.; Liu, J.-g. *Multi-scale Phenomena in Complex Fluids: Modeling, Analysis and Numerical Simulations*; World Scientific Publishing Company: Singapore, 2009.
- (124) Hyon, Y.; Carrillo, J. A.; Du, Q.; Liu, C. *Kinetic and Related Models* **2008**, *1*, 171.
- (125) Hyon, Y.; Du, Q.; Liu, C. *Journal of Computational and Theoretical Nanoscience* **2010**, *7*, 756.
- (126) Ryham, R. J. An Energetic Variational Approach to Mathematical Modeling of Charged Fluids, Charge Phases, Simulation and Well Posedness, Ph.D. Thesis. Ph.D., The Pennsylvania State University, 2006.
- (127) Xu, X.; Liu, C.; Qian, T. *Communications in Mathematical Sciences* **2012**, *10*, 1027.
- (128) Ryham, R.; Cohen, F.; Eisenberg, R. S. *Communications in Mathematical Sciences* **2012**, (in the press).
- (129) Dan, B.-Y.; Andelman, D.; Harries, D.; Podgornik, R. *Journal of Physics: Condensed Matter* **2009**, *21*, 424106.
- (130) Malasics, A.; Gillespie, D.; Boda, D. *Journal of Chemical Physics* **2008**, *128*, 124102.
- (131) Bruna, M.; Chapman, S. J. *Physical Review E* **2012**, *85*, 011103.
- (132) Streetman, B. G. *Solid State Electronic Devices*, 4th ed.; Prentice Hall: Englewood Cliffs, NJ, 1972.
- (133) Sze, S. M. *Physics of Semiconductor Devices*; John Wiley & Sons: New York, 1981.
- (134) Selberherr, S. *Analysis and Simulation of Semiconductor Devices*; Springer-Verlag: New York, 1984.
- (135) Markowich, P. A.; Ringhofer, C. A.; Schmeiser, C. *Semiconductor Equations*; Springer-Verlag: New York, 1990.
- (136) Jerome, J. W. *Analysis of Charge Transport. Mathematical Theory and Approximation of Semiconductor Models*; Springer-Verlag: New York, 1995.
- (137) Howe, R. T.; Sodini, C. G. *Microelectronics: an integrated approach*; Prentice Hall: Upper Saddle River, NJ USA, 1997.
- (138) Hess, K. *Advanced Theory of Semiconductor Devices*; IEEE Press: New York, 2000.
- (139) Berti, C.; Gillespie, D.; Eisenberg, R. S.; Fiegna, C. *Nanoscale Research Letters* **2012**, (in the press).

- (140) Eisenberg, B. *Proceedings of the National Academy of Sciences* **2008**, *105*, 6211.
- (141) Eisenberg, B. available on <http://arxiv.org/> as q-bio/0506016v2 24 pages **2005**.
- (142) Eisenberg, B. *Journal of Computational Electronics* **2003**, *2*, 245.
- (143) Barcion, V.; Chen, D.-P.; Eisenberg, R. S.; Jerome, J. W. *SIAM J. Appl. Math.* **1997**, *57*, 631.
- (144) Chen, D.; Eisenberg, R.; Jerome, J.; Shu, C. *Biophysical J.* **1995**, *69*, 2304.
- (145) Chen, D. P.; Eisenberg, R. S. *Biophys. J* **1993**, *64*, 1405.
- (146) Chen, D. P.; Barcion, V.; Eisenberg, R. S. *Biophys J* **1992**, *61*, 1372.
- (147) Abaid, N.; Eisenberg, R. S.; Liu, W. *SIAM Journal of Applied Dynamical Systems* **2008**, *7*, 1507.
- (148) Eisenberg, B.; Liu, W. *SIAM Journal on Mathematical Analysis* **2007**, *38*, 1932.
- (149) Vasileska, D.; Goodnick, S. M.; Klimeck, G. *Computational Electronics: Semiclassical and Quantum Device Modeling and Simulation*; CRC Press: New York, 2010.
- (150) Kong, C. L. *J Chem Phys* **1973**, *59*, 2464.
- (151) Cazade, P. A.; Dweik, J.; Coasne, B.; Henn, F.; Palmeri, J. *The Journal of Physical Chemistry C* **2010**, *114*, 12245.
- (152) Lakatos, G.; Patey, G. N. *J Chem Phys* **2007**, *126*, 024703.
- (153) Horng, T.-L.; Teng, C.-H. *Journal of Computational Physics* **2012**, *231*, 2498.
- (154) Temes, G. C.; Barcion, V.; Marshall, F. C. *Proceedings of the IEEE* **1973**, *61*, 196.
- (155) Lee, C. C.; Hyon, Y.; Lin, T. C.; Liu, C. (in preparation) **2012**.
- (156) Boda, D.; Henderson, D.; Eisenberg, B.; Gillespie, D. *J Chem Phys* **2011**, *135*, 064105.
- (157) Singer, A.; Gillespie, D.; Norbury, J.; Eisenberg, R. S. *European Journal of Applied Mathematics* **2008**, *19*, 541.
- (158) Howard, J. J.; Perkyons, J. S.; Pettitt, B. M. *The journal of physical chemistry. B* **2010**, *114*, 6074.
- (159) Varsos, K.; Luntz, J.; Welsh, M.; Sarabandi, K. *Proceedings of the IEEE* **2011**, *99*, 2112.
- (160) Fiedziuszko, S. J.; Hunter, I. C.; Itoh, T.; Kobayashi, Y.; Nishikawa, T.; Stitzer, S.; Wakino, K. *IEEE Transactions on Microwave Theory and Techniques* **2002**, *50*, 706.
- (161) Helfferich, F. *Ion Exchange (1995 reprint)*; McGraw Hill reprinted by Dover: New York, 1962.
- (162) Shur, M. *Physics of Semiconductor Devices*; Prentice Hall: New York, 1990.
- (163) Collins, A.; Somlyo, A. V.; Hilgemann, D. W. *J Physiol* **1992**, *454*, 27.
- (164) Hilgemann, D. W.; Collins, A.; Matsuoka, S. *J Gen Physiol* **1992**, *100*, 933.
- (165) Hilgemann, D. W.; Matsuoka, S.; Nagel, G. A.; Collins, A. *J Gen Physiol* **1992**, *100*, 905.
- (166) Matsuoka, S.; Hilgemann, D. W. *J Gen Physiol* **1992**, *100*, 963.
- (167) Schuss, Z.; Nadler, B.; Eisenberg, R. S. *Phys Rev E Stat Nonlin Soft Matter Phys* **2001**, *64*, 036116.
- (168) Schuss, Z.; Nadler, B.; Singer, A.; Eisenberg, R. "A PDE formulation of non-equilibrium statistical mechanics for ionic permeation," AIP Conference Proceedings , 3-6 September 2002: Unsolved Problems Of Noise And Fluctuations, UPoN 2002, 3rd International Conference on Unsolved Problems of Noise and Fluctuations in Physics, Biology, and High Technology 2002, Washington, DC,.

- (169) Hünenberger, P. H.; Reif, M. *Single-Ion Solvation*; RSC Publishing: Cambridge UK, 2011.
- (170) Ben-Naim, A. *Molecular Theory of Water and Aqueous Solutions Part II: The Role of Water in Protein Folding, Self-Assembly and Molecular Recognition* World Scientific Publishing Company, 2011.
- (171) Fraenkel, D. *Molecular Physics* **2010**, *108*, 1435
- (172) Hodgkin, A. L.; Huxley, A. F. *J. Physiol.* **1952**, *116*, 449.
- (173) Hodgkin, A. L.; Huxley, A. F. *J. Physiol.* **1952**, *116*, 473.
- (174) Mullins, L. J. *J. Gen. Physiol.* **1968**, *52*, 555.
- (175) Mullins, L. J. *J. Gen. Physiol.* **1968**, *52*, 550.
- (176) Moore, J. W.; Blaustein, M. P.; Anderson, N. C.; Narahashi, T. *J. Gen. Physiol.* **1967**, *50*, 1401.
- (177) Moore, J. W.; Narahashi, T.; Anderson, N. C.; Blaustein, M. P.; Watanabe, A.; Tasaki, I.; Singer, I.; Lerman, L. *Science* **1967**, *157*, 220.
- (178) Conley, E. C. *The Ion Channel Facts Book. I. Extracellular Ligand-gated Channels*; Academic Press: New York, 1996; Vol. 1.
- (179) Conley, E. C. *The Ion Channel Facts Book. II. Intracellular Ligand-gated Channels*; Academic Press: New York, 1996; Vol. 2.
- (180) Unwin, N. *J Mol Biol* **2005**, *346*, 967.
- (181) Kraus, C. A. *Bull. Amer. Math. Soc.* **1938**, *44*, 361.
- (182) Harned, H. S.; Owen, B. B. *The Physical Chemistry of Electrolytic Solutions*, Third ed.; Reinhold Publishing Corporation: New York, 1958.
- (183) Friedman, H. L. *Ionic Solution Theory*; Interscience Publishers: New York, 1962.
- (184) Rice, S. A.; Gray, P. *Statistical Mechanics of Simple Fluids*; Interscience (Wiley): New York, 1965.
- (185) Barlow, C. A., Jr.; Macdonald, J. R. Theory of Discreteness of Charge Effects in the Electrolyte Compact Double Layer. In *Advances in Electrochemistry and Electrochemical Engineering, Volume 6*; Delahay, P., Ed.; Interscience Publishers: New York, 1967; Vol. VI; pp 1.
- (186) Resibois, P. M. V. *Electrolyte Theory*; Harper & Row: New York, 1968.
- (187) Conway, B. E. *Electrochemical Data*; Greenwood Press Publishers: Westport CT USA, 1969.
- (188) Barker, J.; Henderson, D. *Reviews of Modern Physics* **1976**, *48*, 587.
- (189) Ben-Naim, A. *Inversion of the Kirkwood Buff theory of solutions: Application to the water ethanol system*; AIP, 1977; Vol. 67.
- (190) Pytkowicz, R. M. *Activity Coefficients in Electrolyte Solutions*; CRC: Boca Raton FL USA, 1979; Vol. 1.
- (191) Torrie, G. M.; Valleau, A. *Journal of Physical Chemistry* **1982**, *86*, 3251.
- (192) Hovarth, A. L. *Handbook of aqueous electrolyte solutions: physical properties, estimation, and correlation methods*; Ellis Horwood,: New York, 1985.
- (193) Patwardhan, V. S.; Kumar, A. *AIChE Journal* **1986**, *32*, 1429.
- (194) Stell, G.; Joslin, C. G. *Biophys J* **1986**, *50*, 855.

- (195) Zemaitis, J. F., Jr.; Clark, D. M.; Rafal, M.; Scrivner, N. C. *Handbook of Aqueous Electrolyte Thermodynamics*; Design Institute for Physical Property Data, American Institute of Chemical Engineers: New York, 1986.
- (196) Lee, L. L. *Molecular Thermodynamics of Nonideal Fluids* Butterworth-Heinemann: New York, 1988.
- (197) Pitzer, K. S. *Activity Coefficients in Electrolyte Solutions*; CRC Press: Boca Raton FL USA, 1991.
- (198) Cabezas, H.; O'Connell, J. P. *Industrial & Engineering Chemistry Research* **1993**, *32*, 2892.
- (199) Patwardhan, V. S.; Kumar, A. *AIChE Journal* **1993**, *39*, 711.
- (200) Chhah, A.; Bernard, O.; Barthel, J. M. G.; Blum, L. *Ber. Bunsenges. Phys. Chem.* **1994**, *98*, 1516.
- (201) Hunenberger, P. H.; McCammon, J. A. *J Chem Phys* **1999**, *110*, 1856.
- (202) Baker, N. A.; Hunenberger, P. H.; McCammon, J. A. *J Chem Phys* **2000**, *113*, 2510.
- (203) Durand-Vidal, S.; Simonin, J.-P.; Turq, P. *Electrolytes at Interfaces*; Kluwer: Boston, 2000.
- (204) Kumar, P. V.; Maroncelli, M. *J Chem Phys* **2000**, *112*, 5370.
- (205) Heinz, T. N.; van Gunsteren, W. F.; Hunenberger, P. H. *J Chem Phys* **2001**, *115*, 1125.
- (206) Abbas, Z.; Gunnarsson, M.; Ahlberg, E.; Nordholm, S. *The Journal of Physical Chemistry B* **2002**, *106*, 1403.
- (207) Laidler, K. J.; Meiser, J. H.; Sanctuary, B. C. *Physical Chemistry*, Fourth ed.; Brooks/Cole, Belmont CA, 2003.
- (208) Kastenholtz, M. A.; Hunenberger, P. H. *J Chem Phys* **2006**, *124*, 124106.
- (209) Kornyshev, A. A. *J. Phys. Chem. B* **2007**, *111*, 5545.
- (210) Che, J.; Dzubiella, J.; Li, B.; McCammon, J. A. *J Phys Chem B* **2008**, *112*, 3058.
- (211) Henderson, D.; Boda, D. *Physical Chemistry Chemical Physics* **2009**, *11*, 3822.
- (212) Horinek, D.; Mamatkulov, S.; Netz, R. *J Chem Phys* **2009**, *130*, 124507.
- (213) Ibarra-Armenta, J. G.; Martin-Molina, A.; Quesada-Perez, M. *Physical Chemistry Chemical Physics* **2009**, *11*, 309.
- (214) Janecek, J.; Netz, R. R. *J Chem Phys* **2009**, *130*, 074502.
- (215) Kalcher, I.; Dzubiella, J. *J Chem Phys* **2009**, *130*, 134507.
- (216) Li, B. *Nonlinearity* **2009**, *22*, 811.
- (217) Li, B. *SIAM Journal on Mathematical Analysis* **2009**, *40*, 2536.
- (218) Luo, Y.; Roux, B. t. *The Journal of Physical Chemistry Letters* **2009**, *1*, 183.
- (219) Maginn, E. J. *AIChE Journal* **2009**, *55*, 1304.
- (220) Kalcher, I.; Schulz, J. C. F.; Dzubiella, J. *Physical Review Letters* **2010**, *104*, 097802.
- (221) Kalyuzhnyi, Y. V.; Vlachy, V.; Dill, K. A. *Physical Chemistry Chemical Physics* **2010**, *12*, 6260.
- (222) Lipparini, F.; Scalmani, G.; Mennucci, B.; Cancès, E.; Caricato, M.; Frisch, M. J. *J Chem Phys* **2010**, *133*, 014106.
- (223) Sala, J.; Guardia, E.; Marti, J. *J Chem Phys* **2010**, *132*, 214505.
- (224) Vincze, J.; Valisko, M.; Boda, D. *J Chem Phys* **2010**, *133*, 154507.

- (225) Yu, H.; Whitfield, T. W.; Harder, E.; Lamoureux, G.; Vorobyov, I.; Anisimov, V. M.; MacKerell, A. D.; Roux, B. t. *Journal of Chemical Theory and Computation* **2010**, *6*, 774.
- (226) Zhang, C.; Raugei, S.; Eisenberg, B.; Carloni, P. *Journal of Chemical Theory and Computation* **2010**, *6*, 2167.
- (227) Bazant, M. Z.; Storey, B. D.; Kornyshev, A. A. *Physical Review Letters* **2011**, *106*, 046102.
- (228) Gee, M. B.; Cox, N. R.; Jiao, Y.; Benteinitis, N.; Weerasinghe, S.; Smith, P. E. *Journal of Chemical Theory and Computation* **2011**, null.
- (229) Xiao, T.; Song, X. *J Chem Phys* **2011**, *135*, 104104.
- (230) Zheng, Q.; Chen, D.; Wei, G.-W. *Journal of Computational Physics* **2011**, *230*, 5239.
- (231) Boron, W.; Boulpaep, E. *Medical Physiology*; Saunders: New York, 2008.
- (232) Heras, J. A. *American Journal of Physics* **2007**, *75*, 652.
- (233) Heras, J. A. *American journal of physics* **2008**, *76*, 101.
- (234) Heras, J. A. *Am. J. Phys.* **2011**, *79*, 409.
- (235) Hladky, S. B.; Haydon, D. A. *Nature* **1970**, *225*, 451.
- (236) Sigworth, F. J.; Neher, E. *Nature* **1980**, *287*, 447.
- (237) Hamill, O. P.; Marty, A.; Neher, E.; Sakmann, B.; Sigworth, F. J. *Pflugers Arch* **1981**, *391*, 85.
- (238) FitzHugh, R. *Math. Biosciences* **1983**, *64*, 75.
- (239) Conley, E. C.; Brammar, W. J. *The Ion Channel Facts Book IV: Voltage Gated Channels*; Academic Press: New York, 1999.
- (240) Conley, E. C.; Brammar, W. J. *The Ion Channel Facts Book III: Inward Rectifier and Intercellular Channels* Academic Press: New York, 2000.
- (241) Cherny, V. V.; Murphy, R.; Sokolov, V.; Levis, R. A.; DeCoursey, T. E. *The Journal of General Physiology* **2003**, *121*, 615.
- (242) Levis, R. A.; Rae, J. L. Constructing a patch clamp setup. In *Methods in Enzymology*; Iverson, L., Rudy, B., Eds.; Academic Press: NY, 1992; Vol. 207; pp 66.
- (243) Levis, R. A.; Rae, J. L. *Methods Enzymol* **1998**, *293*, 218.
- (244) Tang, J.; Levis, R.; Lynn, K.; Eisenberg, B. *Biophysical Journal* **1995**, *68*, A145.
- (245) Miodownik-Aisenberg, J. Gating kinetics of a calcium-activated potassium channel studied at subzero temperatures . , University of Miami Medical School, 1995.
- (246) Miller, C. *Ion Channel Reconstitution*; Plenum Press: New York, 1986.
- (247) Miceli, F.; Vargas, E.; Bezanilla, F.; Tagliatalata, M. *Biophysical Journal* **2012**, *102*, 1372.
- (248) Dekel, N.; Priest, M. F.; Parnas, H.; Parnas, I.; Bezanilla, F. *Proc Natl Acad Sci U S A* **2012**, *109*, 285.
- (249) Vargas, E.; Bezanilla, F.; Roux, B. *Neuron* **2011**, *72*, 713.
- (250) Lacroix, J. J.; Bezanilla, F. *Proc Natl Acad Sci U S A* **2011**, *108*, 6444.
- (251) Lacroix, J.; Halaszovich, C. R.; Schreiber, D. N.; Leitner, M. G.; Bezanilla, F.; Oliver, D.; Villalba-Galea, C. A. *J Biol Chem* **2011**, *286*, 17945.

- (252) Vandenberg, C. A.; Bezanilla, F. *Biophys J* **1991**, *60*, 1511.
- (253) Vandenberg, C. A.; Bezanilla, F. *Biophys J* **1991**, *60*, 1499.
- (254) Rae, J. L.; Levis, R. A. *Pflugers Arch* **1992**, *420*, 618.
- (255) Levis, R. A.; Rae, J. L. *Biophys J* **1993**, *65*, 1666.
- (256) Levis, R. A.; Rae, J. L. Technology of patch clamp recording electrodes. In *Patch-clamp Applications and Protocols*; Walz, W., Boulton, A., Baker, G., Eds.; Humana Press.: Totowa, NJ, 1995.
- (257) Doyle, D. A.; Cabral, J. M.; Pfuetschner, R. A.; Kuo, A.; Gulbis, J. M.; Cohen, S. L.; Chait, B. T.; MacKinnon, R. *Science* **1998**, *280*, 69.
- (258) MacKinnon, R. *Angew Chem Int Ed Engl* **2004**, *43*, 4265.
- (259) Schmidt, D.; Cross, S. R.; MacKinnon, R. *J Mol Biol* **2009**, *390*, 902.
- (260) Jimenez-Morales, D.; Liang, J.; Eisenberg, B. *European Biophysics Journal* **2012**, *41*, 449.
- (261) Lutz, S. *Science* **2010**, *329*, 285.
- (262) Ringe, D.; Petsko, G. A. *Science* **2008**, 1428.
- (263) Warshel, A. *J Biol Chem* **1998**, *273*, 27035.
- (264) Dixon, M.; Webb, E. C. *Enzymes*; Academic Press: New York, 1979.
- (265) Martin, P. A. *Reviews of Modern Physics* **1988**, *60*, 1075.
- (266) Henderson, J. R. Statistical Mechanical Sum Rules. In *Fundamentals of Inhomogeneous Fluids*; Henderson, D., Ed.; Marcel Dekker: New York, 1992; pp 23.
- (267) Fuoss, R. M.; Kraus, C. A. *Journal of the American Chemical Society* **1933**, *55*, 2387.
- (268) Fuoss, R. M. *Chemical Reviews* **1935**, *17*, 27.
- (269) Fuoss, R. M.; Onsager, L. *Proc Natl Acad Sci U S A* **1955**, *41*, 274.
- (270) Fuoss, R. M.; Onsager, L. *J Phys Chem B* **1958**, *62*, 1339.
- (271) Fuoss, R. M. *J Phys Chem B* **1959**, *63*, 633.
- (272) Fuoss, R. M.; Onsager, L. *J Phys Chem B* **1962**, *66*, 1722.
- (273) Fuoss, R. M.; Onsager, L. *J Phys Chem B* **1962**, *66*, 1722.
- (274) Fuoss, R. M.; Onsager, L. *J Phys Chem B* **1963**, *67*, 621.
- (275) Fuoss, R. M.; Onsager, L. *J Phys Chem B* **1963**, *67*, 628.
- (276) Fuoss, R. M.; Onsager, L. *J Phys Chem B* **1964**, *68*, 1.
- (277) Fuoss, R. M.; Onsager, L.; Skinner, J. F. *J Phys Chem B* **1965**, *69*, 2581.
- (278) Justice, J.-C. Conductance of Electrolyte Solutions. In *Comprehensive Treatise of Electrochemistry Volume 5 Thermodynamic and Transport Properties of Aqueous and Molten Electrolytes*; Conway, B. E., Bockris, J. O. M., Yeager, E., Eds.; Plenum: New York, 1983; pp 223.
- (279) Csanyi, E.; Boda, D.; Gillespie, D.; Kristof, T. *Biochimica et Biophysica Acta* **2012**, *1818*, 592.
- (280) Boda, D.; Gillespie, D. *Journal of Chemical Theory and Computation* **2012**, *8*, 824.
- (281) Rutkai, G. b.; Boda, D.; Kristóf, T. s. *The Journal of Physical Chemistry Letters* **2010**, *1*, 2179.
- (282) Damocles. *Damocles Web Site, IBM Research*. In

<http://www.research.ibm.com/DAMOCLES/home.html>, 2007.

- (283) Lundstrom, M. *Fundamentals of Carrier Transport*, Second Edition ed.; Addison-Wesley: NY, 2000.
- (284) Jacoboni, C.; Lugli, P. *The Monte Carlo Method for Semiconductor Device Simulation*; Springer Verlag: New York, 1989.
- (285) Eisenberg, R. S.; Kłosek, M. M.; Schuss, Z. *J. Chem. Phys.* **1995**, *102*, 1767 □1780.
- (286) Kłosek, M. M. *Journal of Statistical Physics* **1995**, *79*, 313.
- (287) Segel, I. H. *Enzyme Kinetics: Behavior and Analysis of Rapid Equilibrium and Steady-State Enzyme Systems*, Enzyme Kinetics: Behavior and Analysis of Rapid Equilibrium and Steady-State Enzyme Systems ed.; Wiley: Interscience: New York, 1993.
- (288) Tosteson, D. *Membrane Transport: People and Ideas*; American Physiological Society: Bethesda MD, 1989.
- (289) van der Straaten, T. A.; Tang, J. M.; Ravaioli, U.; Eisenberg, R. S.; Aluru, N. R. *Journal of Computational Electronics* **2003**, *2*, 29.
- (290) Eisenberg, B. *Accounts of Chemical Research* **1998**, *31*, 117.
- (291) Lu, B.; McCammon, J. A. *Chem Phys Lett* **2008**, *451*, 282.
- (292) Vora, T.; Corry, B.; Chung, S. H. *Biochim Biophys Acta* **2006**, *1758*, 730.
- (293) Mamonov, A. B.; Kurnikova, M. G.; Coalson, R. D. *Biophys Chem* **2006**, *124*, 268.
- (294) Corry, B.; Vora, T.; Chung, S. H. *Biochim Biophys Acta* **2005**, *1711*, 72.
- (295) Cardenas, A. E.; Coalson, R. D.; Kurnikova, M. G. *Biophysical Journal* **2000**, 79.
- (296) Berti, C.; Gillespie, D.; Eisenberg, B.; Furini, S.; Fiegna, C. *Biophysical Journal* **2011**, *100*, 158a.
- (297) Eisenberg, R. S. *Journal of Membrane Biology* **1990**, *115*, 1.
- (298) Griffiths, J.; Sansom, C. *The Transporter Facts Book* Academic Press: New York, 1997.
- (299) Jacob, F. *The Logic of Life*; Pantheon; Princeton University Press, 1973 (1993).
- (300) Monod, J. *Chance and Necessity: An Essay on the Natural Philosophy of Modern Biology*; Vintage, 1972.
- (301) Schrödinger, E. *What Is Life?*; Cambridge University Press: New York, 1992.
- (302) Shockley, W. *Electrons and Holes in Semiconductors to applications in transistor electronics*; van Nostrand: New York, 1950.
- (303) Van Roosbroeck, W. *Bell System Technical Journal* **1950**, *29*, 560.
- (304) Gummel, H. K. *IEEE Trans. Electron Devices* **1964**, *ED-11*, 445.